2018

Non-canonical opioid signaling inhibits itch transmission in the spinal cord of mice

Admire Munanairi
Washington University School of Medicine in St. Louis

Xian-Yu Liu
Washington University School of Medicine in St. Louis

Devin M. Barry
Washington University School of Medicine in St. Louis

Qianyi Yang
Washington University School of Medicine in St. Louis

Jun-Bin Yin
Washington University School of Medicine in St. Louis

See next page for additional authors

Article

Cell Reports

Non-canonical Opioid Signaling Inhibits Itch Transmission in the Spinal Cord of Mice

Graphical Abstract

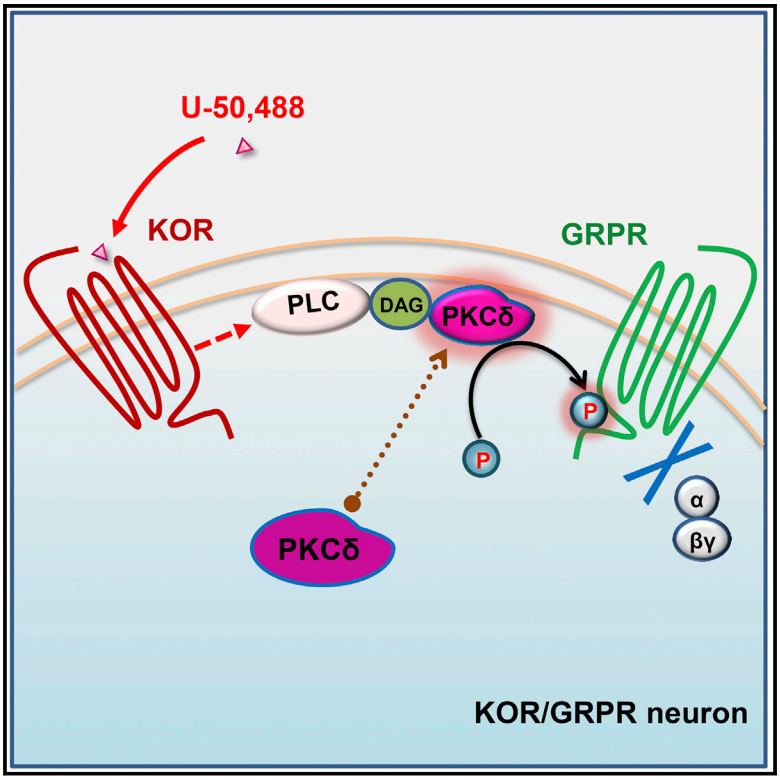

Authors

Admire Munanairi, Xian-Yu Liu, Devin M. Barry, ..., Rita Bardoni, Michael R. Bruchas, Zhou-Feng Chen

Correspondence

chenz@wustl.edu

In Brief

Munanairi et al. show that the kappa opioid receptor (KOR) agonists inhibit nonhistaminergic itch transmission by attenuating the function of the gastrin-releasing peptide receptor (GRPR), an itch receptor in the spinal cord. KOR activation causes the translocation of PKCδ from plasma to membrane, which phosphorylates GRPR to dampen itch transmission.

Highlights

- KOR inhibits itch by attenuating GRPR function
- KOR-GRPR cross-talk is independent of $G_{\alpha i}$ signaling
- KOR desensitizes GRPR via PKCδ translocation
- KOR activates PKCδ translocation via PLC signaling

Munanairi et al., 2018, Cell Reports *23*, 866–877
April 17, 2018
https://doi.org/10.1016/j.celrep.2018.03.087

CellPress

OPEN ACCESS
CellPress

Cell Reports
Article

Non-canonical Opioid Signaling Inhibits Itch Transmission in the Spinal Cord of Mice

Admire Munanairi,[1,2,16] Xian-Yu Liu,[1,2,16] Devin M. Barry,[1,2] Qianyi Yang,[1,2] Jun-Bin Yin,[1,2,6] Hua Jin,[1,9] Hui Li,[1,6] Qing-Tao Meng,[1,2,10] Jia-Hang Peng,[1,2] Zhen-Yu Wu,[1,6] Jun Yin,[1,2] Xuan-Yi Zhou,[1,11] Li Wan,[1,6,12] Ping Mo,[1,6,13] Seungil Kim,[1,14] Fu-Quan Huo,[1,15] Joseph Jeffry,[1,2] Yun-Qing Li,[6,8] Rita Bardoni,[7] Michael R. Bruchas,[2,5] and Zhou-Feng Chen[1,2,3,4,17,*]

[1]Center for the Study of Itch, Washington University School of Medicine, St. Louis, MO 63110, USA
[2]Department of Anesthesiology, Washington University School of Medicine, St. Louis, MO 63110, USA
[3]Department of Psychiatry, Washington University School of Medicine, St. Louis, MO 63110, USA
[4]Department of Developmental Biology, Washington University School of Medicine, St. Louis, MO 63110, USA
[5]Department of Neuroscience, Washington University School of Medicine, St. Louis, MO 63110, USA
[6]Department of Anatomy and K. K. Leung Brain Research Centre, The Fourth Military Medical University, 710032 Xi'an, PRC
[7]Department of Biomedical, Metabolic and Neural Sciences, University of Modena and Reggio Emilia, Modena 41125, Italy
[8]Collaborative Innovation Center for Brain Science, Fudan University, Shanghai 200032, PRC
[9]Present address: The First Hospital of Yunnan Province, Kunming, Yunnan 650031, PRC
[10]Present address: Department of Anesthesiology, Renmin Hospital of Wuhan University, Wuhan, Hubei 430060, PRC
[11]Present address: College of Life Sciences, Wuhan University, Wuhan, Hubei 430072, PRC
[12]Present address: Departments of Pain Medicine, The State Key Clinical Specialty in Pain Medicine, The Second Affiliated Hospital, Guangzhou Medical University, Guangzhou, Guangdong 510260, PRC
[13]Present address: Department of Anesthesiology, the Affiliated Nanhai Hospital of Southern Medical University, Foshan, Guangdong 528000, PRC
[14]Present address: Center for Applied Molecular Medicine, University of Southern California, Los Angeles, CA 90033, USA
[15]Present address: Department of Physiology and Pathophysiology, Xi'an Jiaotong University School of Medicine, Xi'an, Shaanxi 710061, PRC
[16]These authors contributed equally
[17]Lead Contact
*Correspondence: chenz@wustl.edu
https://doi.org/10.1016/j.celrep.2018.03.087

SUMMARY

Chronic itch or pruritus is a debilitating disorder that is refractory to conventional anti-histamine treatment. Kappa opioid receptor (KOR) agonists have been used to treat chronic itch, but the underlying mechanism remains elusive. Here, we find that KOR and gastrin-releasing peptide receptor (GRPR) overlap in the spinal cord, and KOR activation attenuated GRPR-mediated histamine-independent acute and chronic itch in mice. Notably, canonical KOR-mediated $G_{\alpha i}$ signaling is not required for desensitizing GRPR function. *In vivo* and *in vitro* studies suggest that KOR activation results in the translocation of Ca^{2+}-independent protein kinase C (PKC)δ from the cytosol to the plasma membrane, which in turn phosphorylates and inhibits GRPR activity. A blockade of phospholipase C (PLC) in HEK293 cells prevented KOR-agonist-induced PKCδ translocation and GRPR phosphorylation, suggesting a role of PLC signaling in KOR-mediated GRPR desensitization. These data suggest that a KOR-PLC-PKCδ-GRPR signaling pathway in the spinal cord may underlie KOR-agonists-induced anti-pruritus therapies.

INTRODUCTION

Chronic itch or pruritus may arise from dysfunction of skin, immune, nervous system, or internal organ metabolism, such as liver and kidney diseases (Ikoma et al., 2006; Paus et al., 2006). Despite recent progress in identifying signaling molecules as potential targets for anti-pruritus therapies (Bautista et al., 2014; Liu and Ji, 2013), much less is known about the central targets for itch (Barry et al., 2018; Bautista et al., 2014). The mu and kappa opioid receptor systems appear to have opposing roles in a wide range of physiological processes (Pan, 1998), including itch transmission (Ballantyne et al., 1988). Most opioids are pruritogens, and morphine-induced pruritus could be a serious unwanted effect of epidural analgesia (Ballantyne et al., 1988; Reich and Szepietowski, 2010). On the other hand, the inhibitory effect of kappa opioid receptor (KOR) agonists, e.g., butorphanol or nalfurafine (TRK-820), on a wide range of itch behaviors has made them attractive drug candidates for treating patients with uremic, cholestatic, and opioid-induced pruritus (Cowan et al., 2015; Kumagai et al., 2010; Lawhorn et al., 1991; Phan et al., 2012; Togashi et al., 2002; Wikström et al., 2005). KOR-agonist-based anti-pruritic therapies, however, may have unwanted side effects, such as insomnia, somnolence, and constipation (Land et al., 2008; Phan et al., 2012). Despite a potential for KOR agonists in anti-itch application, the underlying mechanisms remain poorly understood.

Gastrin-releasing peptide receptor (GRPR) is primarily required for relaying nonhistaminergic itch in the spinal cord (Akiyama et al., 2013; Barry et al., 2018; Liu et al., 2011; Shiratori-Hayashi et al., 2015; Sun and Chen, 2007; Sun et al., 2009). Its endogenous ligand, gastrin-releasing peptide (GRP), is expressed in a subset of dorsal root ganglion (DRG) neurons, which also overlaps with TRPV1 and substance P (SP) (Barry et al., 2016; Takanami et al., 2014; Zhao et al., 2013). GRP in serum, sensory neurons, and GRPR in the spinal cord of mice, monkeys, and humans with chronic itch were upregulated (Choi et al., 2016; Kagami et al., 2013; Lou et al., 2017; Nattkemper et al., 2013; Tirado-Sánchez et al., 2015; Tominaga et al., 2009; Zhao et al., 2013). A blockade of GRPR or GRP markedly diminishes long-lasting itch in various types of mouse models (Lagerström et al., 2010; Shiratori-Hayashi et al., 2015; Zhao et al., 2013). These studies raise the question of whether KOR may inhibit itch in part by blocking GRPR function. Consistent with this possibility, studies have shown that spinal KOR activation inhibits GRP-induced scratching (GIS) (Kardon et al., 2014; Lee and Ko, 2015) and morphine-induced scratching (MIS) (Ko et al., 2003; Sakakihara et al., 2016).

In this study, we investigated whether spinal KOR activation attenuates itch transmission by blocking GRPR signaling in mice. Using several complementary approaches, we have demonstrated that KOR activation inhibits GRPR signaling via a Ca^{2+}-independent phospholipase C (PLC)-protein kinase C (PKC)δ pathway. Our studies may help design spinal KOR-GRPR cross-signaling-based therapeutic strategies to alleviate chronic itch.

RESULTS

Spinal KOR Activation Inhibits Nonhistaminergic Itch

To determine the effect of spinal activation of KOR on itch, scratching behavior was quantified in C57BL/6J mice after intrathecal (i.t.) injection of U-50,488, a selective KOR agonist (Simonin et al., 1998). Consistent with a previous study (Inan and Cowan, 2004), U-50,488 significantly attenuated scratching behavior induced by chloroquine (CQ), an anti-malaria drug with generalized pruritus (Ajayi et al., 1989). By contrast, U-50,488 had no effect on histamine-induced scratching (Figure 1A). Consistently, U-50,488 markedly reduced i.t. GIS, whereas scratching behavior elicited by neuromedin B (NMB), a bombesin-related peptide, which is involved in histaminergic itch (Wan et al., 2017; Zhao et al., 2014b), was not affected (Figure 1A). The attenuated effect of U-50,488 on GIS and CQ scratching was absent in *Oprk1*$^{-/-}$ mice (Figure S1A), indicating that U-50,488 reduced scratching via a KOR-specific manner. There is no difference in scratching behavior induced by GRP or CQ in male versus female mice (data not shown). Furthermore, we observed a significant decrease in CQ-induced scratching after i.t. injection of U-50,488 in female mice (Figure S1B), suggesting a lack of sexual dimorphic properties in itch transmission (Chakrabarti et al., 2010). Finally, we examined the effect of spinal KOR activation on GRPR-dependent chronic itch models (Zhao et al., 2013). i.t. injection of U-50,488 significantly reduced spontaneous scratching in BRAF$^{Nav1.8}$ mice, a genetic model for chronic itch (Figure 1B). U-50,488 also attenuated chronic itch induced by 2,4-dinitrofluorobenzene (DNFB), a model for allergic contact dermatitis (ACD), and in mice with dry skin itch induced by an acetone-ether-water (AEW) treatment (Zhao et al., 2013; Figures 1C and 1D). These observations demonstrate that spinal KOR activation inhibits GRPR-dependent acute and chronic itch.

KOR Inhibits GRPR in a Cell-Autonomous Manner

The finding that KOR activation inhibited GIS prompted us to examine whether KOR inhibits GIS indirectly through inhibitory neural circuits or directly in GRPR neurons, which are primarily excitatory interneurons (Wang et al., 2013). To differentiate between these two possibilities, we first examined whether KOR and GRPR are co-expressed in the spinal cord using dual-labeled RNAscope *in situ* hybridization (ISH) (Wang et al., 2012). *Oprk1* mRNA was detected in ~50% (104/205) of *Grpr* neurons in the superficial dorsal horn (Figures 1E and 1F).

The co-expression of KOR and GRPR raised the possibility that KOR activation may cross-inhibit GRPR in a cell-autonomous manner rather than through activation of inhibitory neural circuits. GRPR transduces itch via the PLCβ/IP_3/Ca^{2+} signaling pathway (Liu et al., 2011; Zhao et al., 2014a). To examine this, the dorsal horn of the spinal cord was dissected and dissociated and neurons were cultured for calcium imaging (Figure 2A; Video S1). To determine whether U-50,488 inhibits GRP-induced, GRPR-mediated intracellular Ca^{2+} mobilization, a two-step protocol was employed, whereby dissociated dorsal horn GRPR$^+$ neurons can be identified by an application of GRP (20 nM) and then re-sensitized after a 30-min wash-out period (Figure 2C; Table S1; Zhao et al., 2014a). The ratio of the second GRP-induced response to the first response was used for quantitation, thereby avoiding inconsistencies that may result from GRPR$^+$ neuronal heterogeneity. U-50,488 (up to 20 μM) alone did not induce Ca^{2+} responses in GRPR$^+$ neurons (data not shown). However, incubation of U-50,488 (10 μM) attenuated Ca^{2+} responses of GRPR$^+$ neurons to GRP (Figures 2B, 2D, and 2F; Video S2), and this inhibitory effect was reversed by norbinaltorphimine (norBNI), a selective KOR antagonist (Portoghese et al., 1987; Figures 2E and 2F). About 42% of GRPR$^+$ neurons showed complete inhibition (52/124) by KOR activation, 26% showed partial inhibition (32/124), and 32% were resistant to U-50,488 application (40/124; Table S2). The finding that the percentage of non-responders was slightly lower than *Grpr*$^+$/*Oprk1*$^-$ neurons, as observed by RNAscope ISH (Figures 1E and 1F), could be due to several factors, such as younger age of mice used for calcium imaging study and/or different sensitivities associated with each approach. CQ itch is significantly reduced, but not abolished, in *Grpr* KO mice (Sun and Chen, 2007), suggesting the involvement of a GRPR-independent pathway. To test whether U-50,488 may inhibit CQ itch via GRPR-independent pathway, we examined its effect on CQ itch using *Grpr* KO mice and found that i.t. U-50,488 did not further reduce CQ-induced scratching (Figure S2A). This result suggests that spinal KOR activation inhibits CQ itch predominantly via GRPR-cell-autonomous mechanism.

Next, we investigated whether KOR activation inhibits GRPR signaling via the canonical opioid-mediated $G_{\alpha i}$ signaling pathway (Al-Hasani and Bruchas, 2011). Unexpectedly,

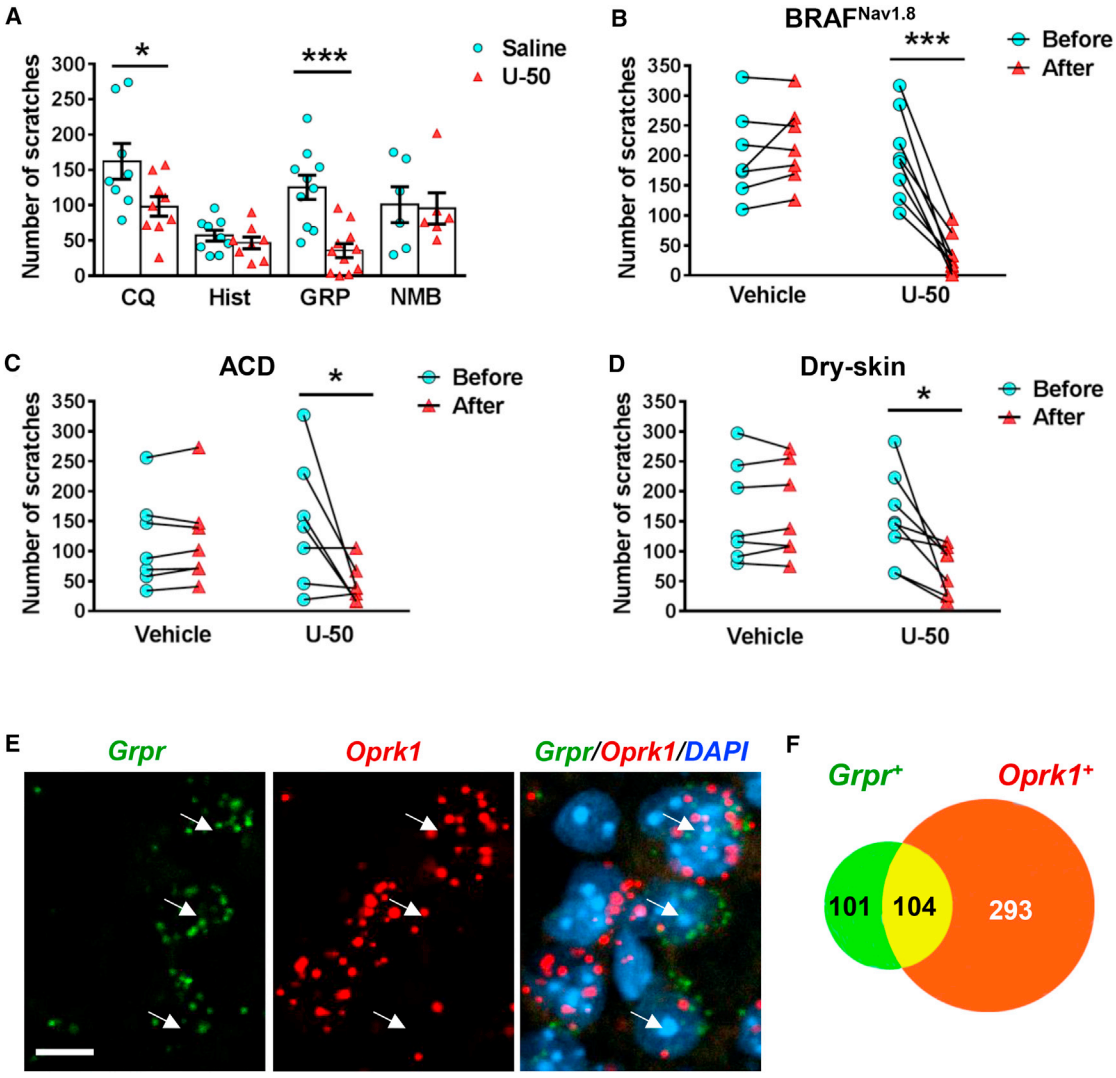

Figure 1. Intrathecal Administration of U-50,488 Attenuates Nonhistaminergic Itch

(A) 10-min pre-injection of U-50,488 (10 nmol) significantly reduced scratching induced by CQ (200 μg intradermal [i.d.]) and GRP (0.3 nmol i.t.), but not Hist (200 μg i.d.) and NMB (1 nmol i.t.; *p < 0.05; ***p < 0.001; Student's unpaired t test; n = 6–11).

(B–D) Reduced spontaneous scratching in (B) $BRAF^{Nav1.8}$, (C) ACD, and (D) dry-skin mice after U-50,488 injection (*p < 0.05; ***p < 0.001; Student's paired t test; n = 7–9).

(E) Representative images of RNAscope *in situ* hybridization of *Grpr* (green) and *Oprk1* (red) mRNA expression in superficial dorsal horn of transverse lumbar sections. Arrows indicate double-stained neurons. Blue represents DAPI nucleic acid stain (scale bar, 20 μm).

(F) Venn diagram showing the overlap in expression of *Grpr* and *Oprk1* in dorsal horn neurons (n = 20 lumbar sections from 3 mice). Data are represented as mean ± SEM.

See also Figures S1 and S2.

pertussis toxin (PTX) (200 ng/mL), a $G_{\alpha i}$ inhibitor, did not block the inhibitory effect of U-50,488 (Figure 2G), suggesting that a $G_{\alpha i}$-independent pathway is involved in spinal KOR activation-mediated itch inhibition. Of the 23 GRPR neurons treated with PTX, GRP-induced calcium responses in 16/23 (70%) were completely inhibited by U-50,488, 2/23 (9%) showed partial inhibition, whereas 5/23 (21%) were resistant to U-50,488 treatment. As expected, PTX reversed U-50,488-mediated inhibition of cyclic AMP (cAMP) synthesis in HEK293 cells (Figure S3A). To test whether KOR may differentially couple to $G_{\alpha s}$ in GRPR-KOR cells, we measured cAMP accumulation and found that neither U-50,488, GRP, nor their co-application induced cAMP accumulation (Figure S3B), implying that it is unlikely that a $G_{\alpha s}$-dependent pathway is involved in KOR-GRPR cross-signaling.

According to the canonical pathway, activation of KOR recruits G-protein-coupled receptor kinases (GRK). Arrestin will then bind to the phosphorylated KOR, resulting in acute desensitization (Bruchas and Chavkin, 2010). In contrast, U-50,488-mediated desensitization lasts for at least two days in mice (Figure S1C). Furthermore, U-50,488 attenuated GIS

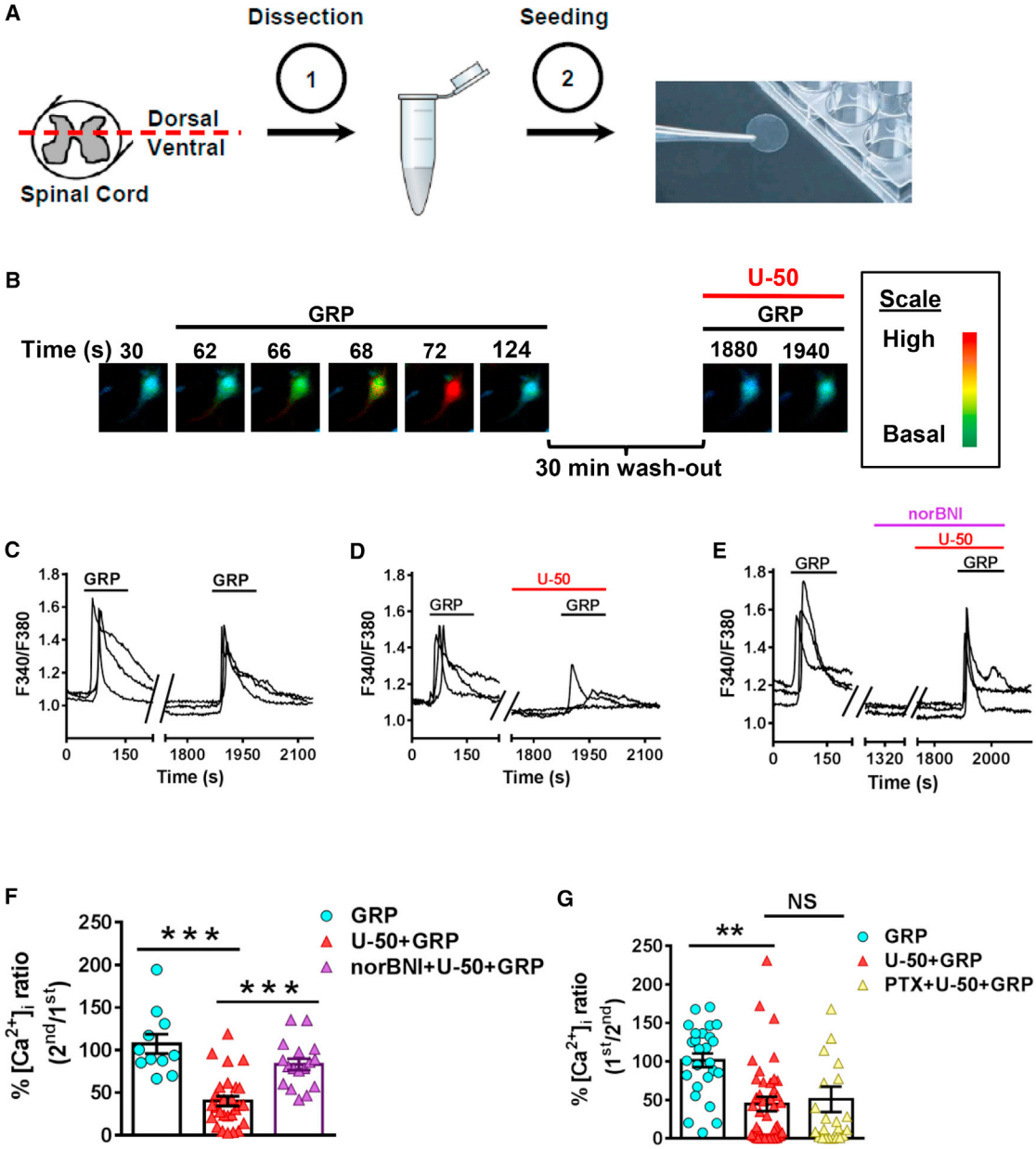

Figure 2. Activation of KOR Inhibits GRPR Ca^{2+} Signaling in Dorsal Horn Neurons

(A) Schematic showing dissection of the spinal cord, seeding, and culture of dissociated dorsal horn neurons.

(B) Ratiometric fluorescence images of dissociated GRPR neurons showing changes in calcium after adding 20 nM GRP (62–124 s). After a wash-out period, a 2-min pretreatment with 10 μM U-50,488 inhibited GRP-induced Ca^{2+} responses in GRPR neurons (1,880–1,940 s).

(C) Representative traces showing that GRP-induced calcium responses completely recovered after a 30-min wash-out period.

(D) U-50,488 inhibited GRP-induced Ca^{2+} responses in dissociated dorsal horn neurons.

(E) 10-min pretreatment with 10 μM norBNI blocked the U-50,488 inhibitory effect on GRP-induced Ca^{2+} responses.

(F) Quantified data comparing peak intracellular concentration evoked by GRP after pretreatment with U-50,488 (red) or norBNI+U-50,488 (purple; ***$p < 0.001$; one way ANOVA followed by Tukey's multiple comparison test; n = 11–27).

(G) PTX (200 ng/mL) had no effect on U-50,488 inhibitory effect on GRP-induced Ca^{2+} responses (**$p < 0.01$; NS, not significant; one way ANOVA followed by Tukey's multiple comparison test; n = 26–49).

Data are represented as mean ± SEM. See also Figures S2 and S3.

in *Arrb2*$^{-/-}$ mice (Figure S3C), consistent with previous studies (Bohn et al., 2000; Morgenweck et al., 2015). Although we cannot completely exclude the involvement of arrestin signaling, due to possible genetic compensation in *Arrb2*$^{-/-}$ mice, the long-lasting effect of KOR-mediated inhibitory action on itch transmission supports the notion that KOR activation

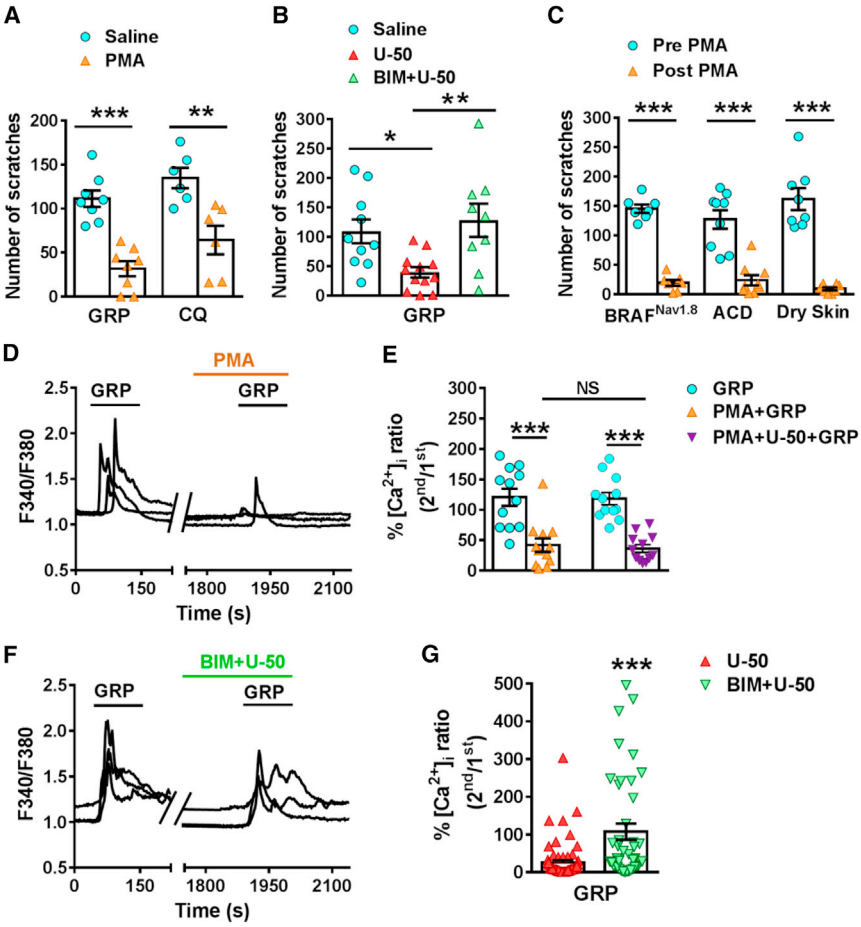

Figure 3. PKC Inhibition in the Spinal Cord Blocks KOR-Activation-Induced Attenuation of Itch

(A) Pre-injection of PMA (1 nmol i.t.) significantly reduced scratching induced by GRP and CQ (**$p < 0.01$; ***$p < 0.001$; Student's unpaired t test; n = 6–8).

(B) BIM (40 pmol i.t.), blocked U-50,488 inhibitory effect on GRP-induced scratching (*$p < 0.05$; **$p < 0.01$; one-way ANOVA followed by Tukey's multiple comparison test; n = 9–12).

(C) PMA (1 nmol) inhibited spontaneous scratching in $BRAF^{Nav1.8}$, ACD, and dry-skin mice (***$p < 0.001$; Student's paired t test; n = 7–9).

(D and E) Representative traces (D) and quantified data (E) show that PMA (1 μM) inhibits GRP-induced Ca^{2+} responses in dissociated GRPR neurons (***$p < 0.001$; Student's unpaired t test; n = 12). The inhibitory effect was no further reduced by co-application of PMA (1 μM) and U-50,488 (10 μM; ***$p < 0.001$; Student's unpaired t test; n = 15).

(F and G) BIM (5 μM) blocked U-50,488 inhibitory effect on GRP-induced Ca^{2+} responses (***$p < 0.001$; Student's unpaired t test; n = 43–65).

Data are represented as mean ± SEM.

attenuates itch through β-arrestin2 signaling-independent pathway.

Spinal KOR Activation Inhibits GRPR Function via a PKC-Dependent Mechanism

Previous *in vitro* studies show that GRPR is a substrate of PKC that phosphorylates and desensitizes GRPR (Ally et al., 2003). To explore the possibility that PKC activation inhibits itch, scratching behavior was examined in mice pre-injected with i.t. phorbol myristate acetate (PMA), a PKC activator (Way et al., 2000), which markedly attenuated CQ-induced scratching and GIS, mimicking the U-50,488 effect (Figure 3A). Interestingly, bisindolylmaleimide (BIM), a selective inhibitor for PKCα, β1, β2, γ, δ, and ε isoforms (Toullec et al., 1991), blocked the effect of U-50,488 on GIS (Figure 3B). Furthermore, PMA completely blocked spontaneous scratching behavior of $BRAF^{Nav1.8}$ mice, ACD, and dry skin chronic itch mouse models (Figure 3C). These findings raised a possibility that KOR activation suppresses itch via PKC-mediated inhibition of GRPR function.

Next, we examined whether PKC activation could reduce GRP-induced Ca^{2+} responses in $GRPR^{+}$ neurons by applying PMA. Consistent with behavioral studies, PMA significantly attenuated GRP-induced Ca^{2+} responses (Figures 3D and 3E). Co-application of PMA and U-50,488 did not further reduce GRP-induced Ca^{2+} responses, suggesting that KOR activation attenuates GRPR signaling via PKC (Figures 3D and 3E). Moreover, pre-incubation with BIM (5 μM) blocked the inhibitory effect of U-50,488 on Ca^{2+} responses of $GRPR^{+}$ neurons (Figures 3F and 3G). These observations support the notion that KOR activation attenuates itch transmission via PKC-mediated inhibition of spinal GRPR function.

Activation of KOR Induces GRPR Phosphorylation via PKC

Whole-cell phosphorylation assays were performed to further elucidate the role of PKC in KOR-activation-induced inhibition of GRPR signaling. In HEK293 cells expressing FLAG-KOR and Myc-GRPR, GRPR phosphorylation increased 13-fold after a 2-min incubation in U-50,488 (10 μM; Figures 4A, 4B, and S7A). Consistent with behavior and calcium-imaging results, PKC inhibition by BIM (5 μM) blocked KOR-activation-induced GRPR phosphorylation (Figures 4C and S7B). Rapid GRPR phosphorylation was also observed within 2 min after treatment with PMA (1 μM) and decreased after 15 min (Figures 4D and S7C), in accordance with previous findings (Ally et al., 2003). Phosphorylation assays showed that U-50,488-mediated KOR activation induces rapid and robust, GRP-independent phosphorylation of GRPR, which may cause desensitization of GRPR activity.

KOR Activation Attenuates Itch via PKCδ

The PKC family consists of a variety of isoforms that can be classified into three sub-families: conventional (α, β1, β2, and γ; Ca^{2+}

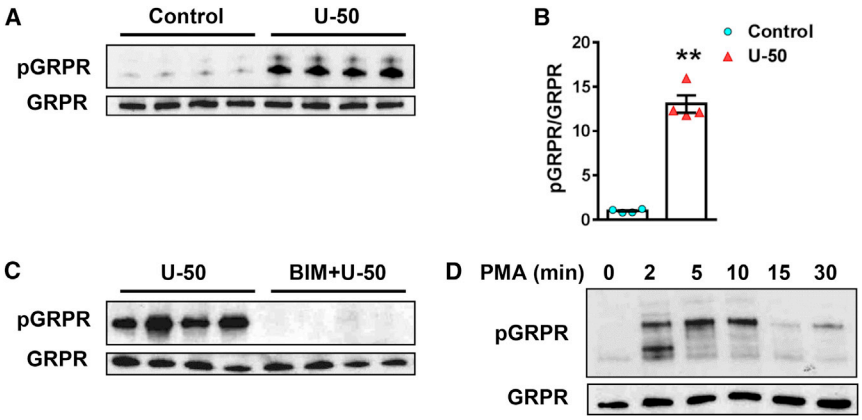

Figure 4. Activation of KOR Induces GRPR Phosphorylation via PKC

(A and B) Western blots (A) and quantified data (B) showing that U-50,488 induced robust GRPR phosphorylation after 2 min in HEK293 cells expressing KOR and GRPR (**$p < 0.01$ Student's paired t test; $n = 4$).

(C) BIM (5 μM) blocked U-50,488-induced phosphorylation of GRPR ($n = 4$).

(D) Time course analysis of PMA (1 μM)-induced GRPR phosphorylation in HEK293 cells.

Data are represented as mean ± SEM. See also Figure S7.

and diacylglycerol [DAG] dependent); novel (δ, ε, η, and θ; DAG dependent); and atypical (ζ and I/λ; Nishizuka, 1995; Steinberg, 2008). Given that U-50,488 failed to induce Ca^{2+} responses in GRPR neurons, we postulated that Ca^{2+}-independent PKC isoforms (PKCδ or ε) may be involved in mediating KOR-dependent PKC activation. To identify the PKC isoform involved, we performed spinal PKC-isoform-specific small interfering RNA (siRNA) knockdown studies (Liu et al., 2011). Remarkably, siRNA knockdown of *Prkcd* not only blocked U-50,488 inhibition of GIS (Figure 5A) but also enhanced CQ-induced itch, even in the presence of U-50,488 (Figure 5B). Treatment of control siRNA did not affect U-50,488 inhibitory effect on GIS and CQ itch (Figures S4A and S4B). qRT-PCR of the lumbar spinal cord confirmed specific knockdown of *Prkcd*, but not *Prkca* (Figure 5C). Consistently, U-50,488 lost effect on GRP-induced calcium responses of dorsal horn neurons isolated from $Prkcd^{-/-}$ mice (Figure S5B). We also performed siRNA knockdown of *Prkca.* However, U-50,488 attenuated CQ-induced itch after siRNA knockdown of *Prkca*, suggesting that PKCα does not mediate KOR activation inhibition of itch (Figures S4C and S4D).

Next, we examined the role of PKCδ in KOR-activation-mediated itch inhibition using $Prkcd^{-/-}$ mice and their wild-type (WT) littermates (Leitges et al., 2001) and did not find differences in GIS between $Prkcd^{-/-}$ and WT littermates. As predicted, the inhibitory effect of U-50,488 on GIS is lost in $Prkcd^{-/-}$ mice relative to their WT littermates (Figure 5D). To examine whether PKCδ is co-expressed with GRPR in the superficial dorsal horn, we generated a $Grpr^{iCre}$/Ai9 reporter mouse line by crossing $Grpr^{iCre}$ mice with a tdTomato Ai9 line. Double immunohistochemistry (IHC) studies were conducted, and PKCδ was detected in $Grpr^{iCre}$-tdTomato^{+} neurons (arrows indicate overlap in expression; Figure 5E). Further, we labeled spinal GRPR neurons with enhanced yellow fluorescent protein (eYFP) by injection of AAV5-Ef1a-DIO-eYFP virus into the dorsal spinal cord of $Grpr^{iCre}$ mice. Consistently, we detected numerous PKCδ in $Grpr^{iCre}$; AAV-DIO-eYFP neurons (Figures 5F and S5A).

KOR Activation Induces PKCδ Translocation to the Plasma Membrane

To further evaluate the role of PKCδ in KOR-activation-induced inhibition of GRPR signaling, we examined PKC translocation from the cytosol to the plasma membrane, a hallmark of PKC activation (Mochly-Rosen et al., 1990). Using GFP-tagged PKC, the dynamics of PKC translocation in response to different stimuli can be monitored in live cells and in real time (Oancea et al., 1998; Wang et al., 1999). HEK293 cells expressing KOR and GRPR were transfected with PKCδ-EGFP or PKCα-EGFP. Confocal live-cell imaging was then performed to characterize spatiotemporal properties of PKCδ-EGFP or PKCα-EGFP after application of U-50,488 or PMA. PKCδ and PKCα were present in the cytosol without stimulation (Figure 6A; 0 min). Application of U-50,488 (10 μM) prompted translocation of PKCδ, but not PKCα, to the cell membrane. PKCδ-EGFP translocation from the cytosol to the plasma membrane was apparent as early as 5 min and reached a maximum after 30 min of incubation in U-50,488 (Figure 6A; Video S3). After U-50,488 treatment, translocation to the plasma membrane increased significantly (from 15% ± 4% to 62% ± 8%; Figure 6B). As expected, direct activation of PKC with PMA (100 nM) induced translocation of both PKCδ-EGFP and PKCα-EGFP from the cytosol to the membrane (Figures 6C and 6D; Video S4).

To evaluate that the U-50,488-induced PKCδ translocation observed in HEK293 cells mimics events *in vivo*, the fraction of PKCδ-positive dorsal horn neurons was quantified 30 min after i.t. injection of U-50,488 in mice. We found that the fraction of dorsal horn neurons with plasma-membrane-bound PKCδ nearly doubled after U-50,488 injection (from 40% ± 1% to 73% ± 2%; Figures 6E–6G). This confirmed that KOR activation stimulates PKCδ activity manifested by its translocation to the plasma membrane, which subsequently phosphorylates and desensitizes GRPR signaling.

KOR Activation Stimulates PKCδ via PLC

To elucidate the mechanism by which KOR activation stimulates PKCδ, we tested a myriad of inhibitors on U-50,488-induced PKCδ translocation in HEK293 cells expressing KOR and GRPR. Pre-incubation of U73122 (10 μM), a PLC inhibitor, for 10 min blocked U-50,488-induced PKCδ-EGFP translocation to the plasma membrane. In contrast, U-50,488 treatment increased the membrane translocation of PKCδ-EGFP from 12% ± 4% to 64% ± 5% in the presence of U73343 (10 μM), an inactive analog of U73122 (Figures 7A and 7B). Furthermore,

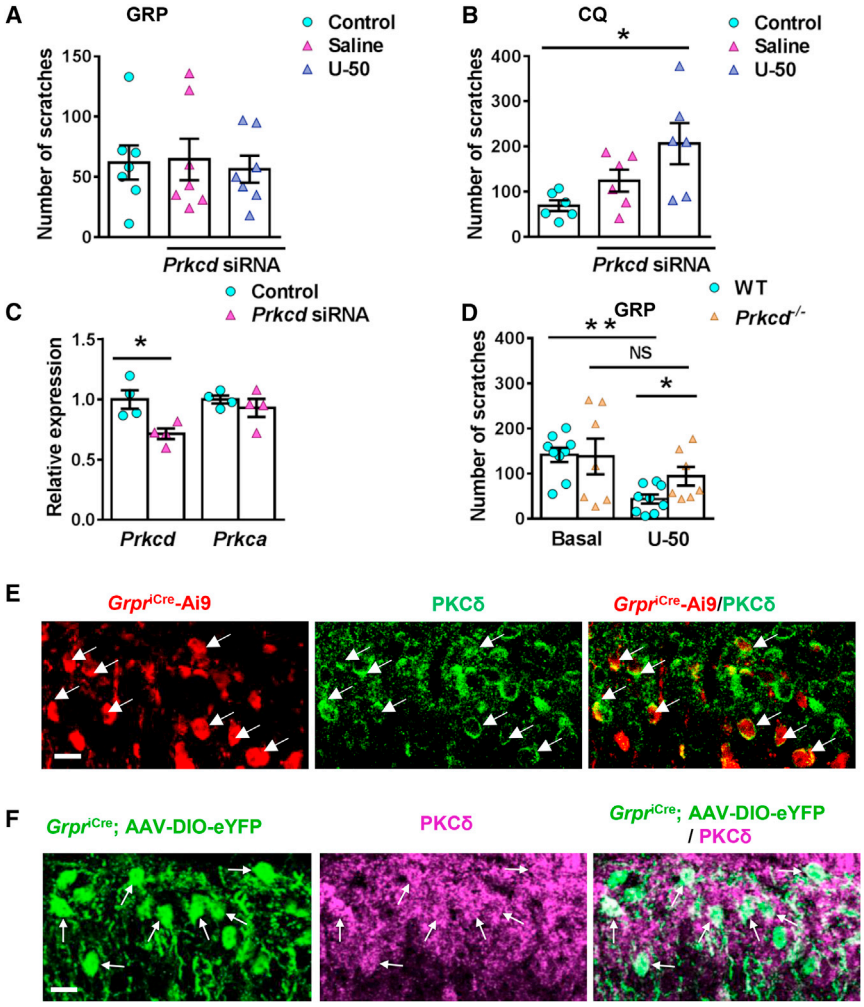

Figure 5. U-50,488 Attenuates Itch via PKCδ

(A and B) U-50,488 failed to block scratching induced by (A) GRP (0.06 nmol i.t.) and (B) CQ (100 μg i.d.) in *Prkcd* siRNA-treated mice (*$p < 0.05$; one way ANOVA followed by Tukey's multiple comparison test; n = 7).

(C) qRT-PCR showed that the level of spinal *Prkcd* mRNA was significantly reduced by *Prkcd* siRNA injection, whereas the *Prkca* mRNA level was not affected (*$p < 0.05$; Student's unpaired t test; n = 4).

(D) U-50,488 failed to block scratching induced by GRP (0.3 nmol i.t.) in *Prkcd*$^{-/-}$ mice (*$p < 0.05$; **$p < 0.01$; Student's unpaired and paired t test; basal relative to U-50; n = 7–9).

(E) Double IHC of tdTomato (red) and PKCδ (green) shows co-expression of GRPR and PKCδ in superficial dorsal horn neurons.

(F) Double IHC of PKCδ (purple) and eYFP (green) shows co-expression of GRPR and PKCδ in superficial dorsal horn neurons of *Grpr*-iCre mice injected with AAV-DIO-eYFP. Arrows indicate double-stained cells. The scale bar represents 10 μm.

Data are represented as mean ± SEM. See also Figure S5.

U-50,488 treatment increased the translocation of PKCδ-EGFP from 11% ± 2% to 47% ± 5% and 15% ± 3% to 70% ± 9% after a prior pre-incubation in gallein (100 μM), a $G_{\beta\gamma}$ inhibitor, and PTX (200 ng/mL), respectively (Figures 7C and 7D), suggesting that PLC mediates PKCδ activation by KOR in a $G_{\beta\gamma}$- and $G_{\alpha i}$-independent process. Whole-cell phosphorylation assays were also used to show that KOR activation induces GRPR phosphorylation via PLC. U73122, but not U73343, blocked GRPR phosphorylation (Figures 7E, 7F, and S7D). Together, these results suggest that KOR activation stimulates PLC, resulting in the translocation of PKCδ from the cytosol to the plasma membrane, where it phosphorylates GRPR (Figure 7G).

To investigate whether this pathway is similarly engaged by other KOR agonists, we tested butorphanol, a mixed KOR agonist/MOR antagonist (Abeliovich et al., 1993), which has been used to treat various types of intractable pruritus in human studies (Dawn and Yosipovitch, 2006; Dunteman et al., 1996). We found that i.t. injection of butorphanol (2 nmol) significantly reduced CQ-induced scratching behaviors in WT, but not in *Oprk1*$^{-/-}$ mice (Figure S2B), suggesting that butorphanol inhibits CQ itch via a KOR-dependent mechanism. Furthermore, i.t. injection of butorphanol (2 nmol) did not further reduce CQ-induced scratching in *Grpr* KO mice (Figure S2C). Consistently, butorphanol also lost effect in *Prkcd*$^{-/-}$ mice (Figure S2D). These studies provide clinically relevant evidence supporting that spinal KOR-agonists-mediated itch inhibition is dependent on the KOR-GRPR cross-talk, but not other mechanisms. In HEK293 cells expressing KOR and GRPR, butorphanol induced PKCδ-EGFP, but not PKCα-EGFP, translocation from the cytosol to the plasma membrane, mimicking the U-50,488 effect (Figure S6). Consistent with U-50,488 and butorphanol results, dynorphin, an endogenous ligand for KOR (Chavkin et al., 1982), also attenuated CQ-induced itch (Figure S2E). However, mice lacking dynorphin (*Pdyn*$^{-/-}$) exhibited normal acute and chronic itch (Figures S2F and S2G). These data demonstrate that spinal KOR activation by different agonists suppresses itch transmission via PLC-PKCδ pathway and endogenous dynorphin is not required for itch modulation under either normal physiological or chronic itch conditions.

DISCUSSION

Using a multidisciplinary and spinal-cord-specific approach, we show that a Ca^{2+}-independent KOR-PLC-PKCδ-GRPR pathway is activated in response to KOR agonists, resulting in an attenuation of GRPR function, which is required for development of chronic itch in mice (Sun and Chen, 2007; Zhao et al., 2013). Consistent with previous findings showing that GRPR is minimally required for histaminergic itch (Akiyama et al., 2014; Sun et al., 2009; Zhao et al., 2013), we show that spinal KOR

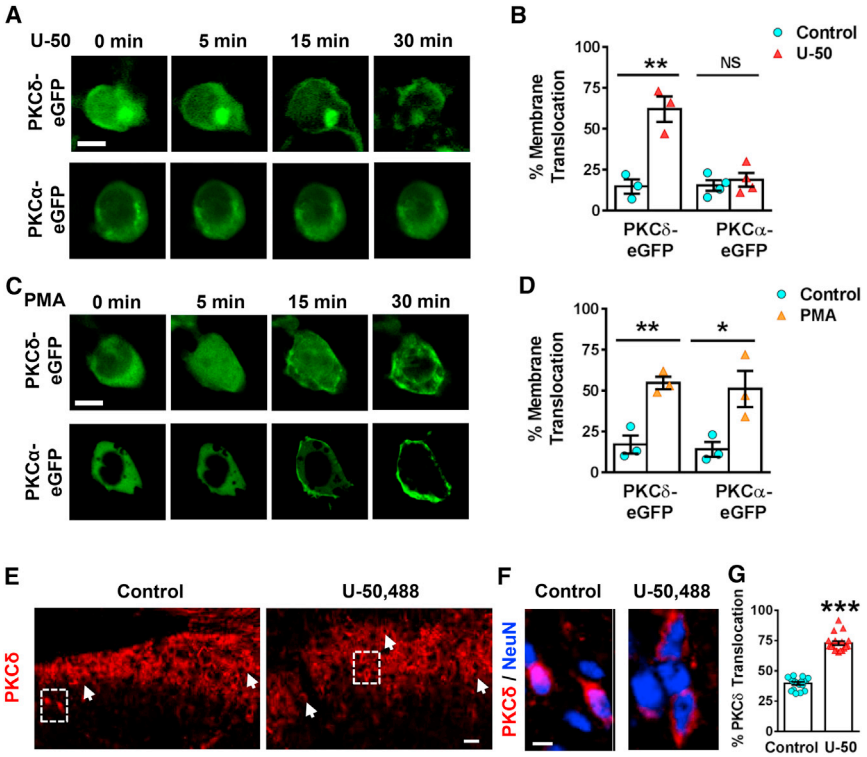

Figure 6. KOR Activation Induces Translocation of PKCδ, but Not PKCα, to the Plasma Membrane

(A) HEK293 cells expressing KOR/GRPR transfected with PKCδ-EGFP (upper row) and PKCα-EGFP (lower row) were incubated in 10 μM U-50,488. Confocal images taken at indicated time points showed that U-50,488 induced the translocation of PKCδ-EGFP, but not PKCα-EGFP, to the plasma membrane (scale bar, 20 μm).

(B) Percentage of PKCδ-EGFP and PKCα-EGFP translocation to the plasma membrane in response to U-50,488 (**p < 0.01; Student's paired t test; n = 3–4 cells per experiment).

(C) 100 nM PMA incubation induced the translocation of both PKCδ-EGFP and PKCα-EGFP to the plasma membrane.

(D) Percentage of PKCδ-EGFP and PKCα-EGFP translocation to the plasma membrane in response to PMA (*p < 0.05; **p < 0.01; Student's paired t test; n = 3–4 cells per experiment).

(E) IHC image shows that PKCδ (red) is mostly distributed in the cytosol of superficial dorsal horn neurons of control mouse (upper row). After U-50,488 injection, PKCδ translocates to the plasma membrane (lower row). Arrows show neurons with PKCδ distributed at the plasma membrane (scale bar, 20 μm).

(F) High-power images of the boxed regions in (E; scale bar, 5 μm; blue, NeuN).

(G) Percentage of PKCδ translocation to the plasma membrane after U-50,488 injection relative to control in dorsal horn neurons (***p < 0.001; Student's unpaired t test; n = 18 lumbar sections from 3 mice).

Data are represented as mean ± SEM. See also Figure S6.

activation does not impact histaminergic itch, including NMB-mediated scratching behavior (Wan et al., 2017; Zhao et al., 2014b). Our data suggest that the anti-histaminergic itch effect elicited by systemic KOR agonists is likely attributable to peripheral KOR (Bigliardi-Qi et al., 2007; Chuang et al., 1995; Suzuki et al., 2001; Togashi et al., 2002). Taken together, these findings illustrate a spinal mechanism by which KOR agonists attenuate itch transmission.

Spinal KOR activation reduces itch transmission by inhibiting the function of GRPR in a cell-autonomous manner in KOR-GRPR neurons. In addition to GRPR excitatory neurons, KOR is also expressed in non-GRPR GABAergic neurons in the spinal cord (Xu et al., 2004). Activation of KOR in non-GRPR neurons by KOR agonists could induce thermal analgesia (Nakazawa et al., 1990; Porreca et al., 1984; Xu et al., 2004), likely via the $G_{\alpha i}$ signaling pathway (Al-Hasani and Bruchas, 2011; Grudt and Williams, 1993; Randić et al., 1995). Because of itch and pain antagonism and their distinct neuronal outputs, it is unlikely that inhibition of non-GRPR KOR neurons in the spinal cord would contribute to itch inhibition. Importantly, KOR-agonist-induced anti-itch effect is lost in *Grpr* KO mice, suggesting that GRPR is required for mediating anti-itch effects. The remaining KOR-agonist-resistant scratching effect induced by CQ in *Grpr* KO mice is likely mediated by glutamatergic transmission in *Grpr*$^{-/-}$ neurons that are also required for histaminergic transmission (Akiyama et al., 2014; Wan et al., 2017). Taken together, depending on GRPR and neurotransmitter expression, activation of KOR neurons in the spinal cord gives rise to two distinct behavioral outputs: GABAergic KOR neurons compute anti-nociceptive output, whereas excitatory KOR-GRPR neurons convey anti-pruriceptive information (Figure 7H). The dual role of KOR is reminiscent of MOR1 and 5HT1A, which is predominantly implicated in anti-nociceptive signaling, with only a small percentage communicating with GRPR, in contrast to KOR-GRPR, to induce or facilitate itch (Liu et al., 2011; Zhao et al., 2014a). Thus, depending on agonists and type of GPCRs, GRPR neurons could serve as a gate to control the output of itch information.

The observation that PTX fails to reverse the effect of U-50,488 demonstrates that KOR signaling via a non-canonic $G_{\alpha i}$-independent pathway, is specific to KOR-GRPR excitatory neurons. The finding that KOR-activation-mediated signal transduction is independent of $G_{\beta\gamma}$ protein as well as $G_{\alpha s}$ protein suggests that KOR may activate PLC independent of G protein. How could KOR activate PKCδ, but not PLCβ, which acts downstream of GRPR (Liu et al., 2011), in GRPR neurons? It is possible that KOR activation selectively recruits PKCδ to phosphorylate GRPR, thereby dampening PLCβ signaling via a competitive manner (Figure 7G). It is also likely that the presence of a GRPR-KOR heteromeric complex switches the downstream signaling kinase cascade of canonic KOR pathway to occlude PLCβ activation.

One remarkable finding is that Ca^{2+}-independent PKCδ activation via membrane translocation provides a major mechanism

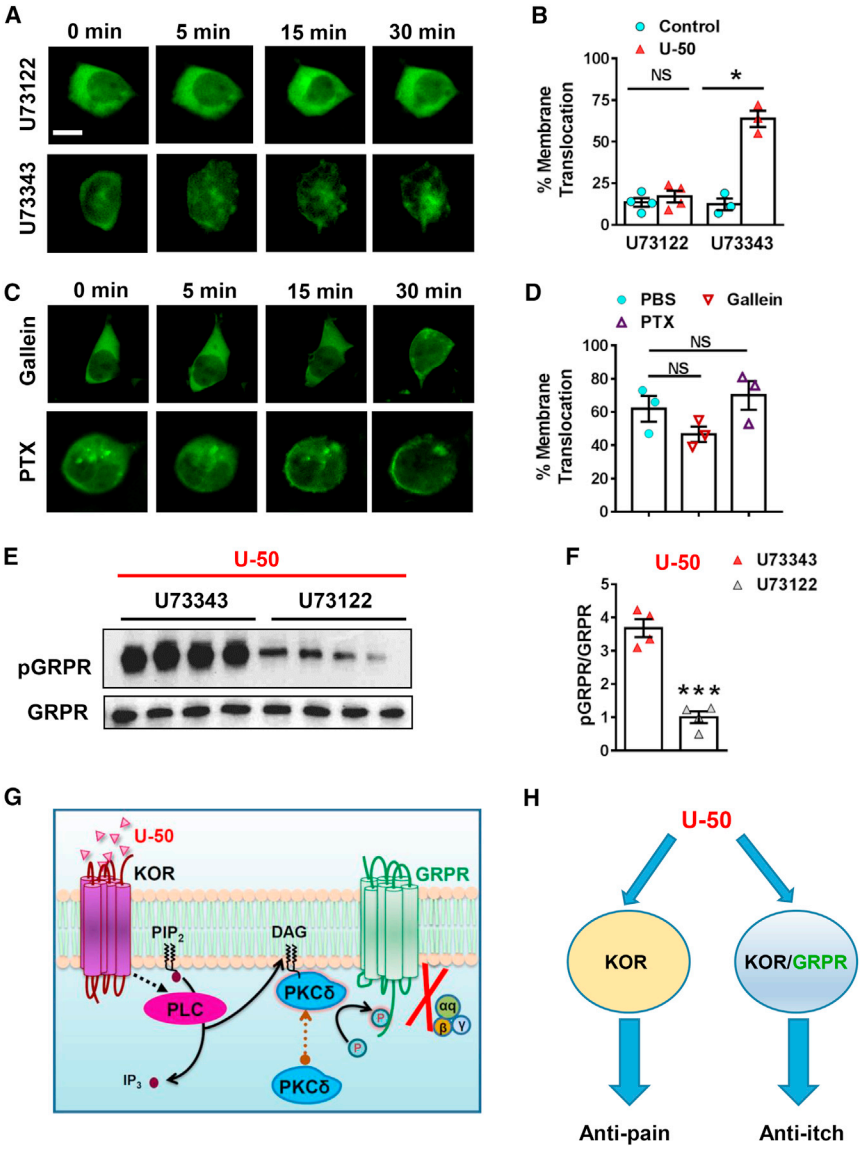

Figure 7. PLC Mediates KOR-Activation-Induced Translocation of PKCδ to the Plasma Membrane

(A–D) Confocal images (A and C) and quantified data (B and D) showing U-50,488 induced translocation of PKCδ-eGFP from the cytosol to the plasma membrane was blocked by 10 μM U73122 (PLC inhibitor) (A and B). U73343 (inactive analog of U73122) (A and B), 100 μM gallein ($G_{\beta\gamma}$ inhibitor), and 200 ng/mL PTX ($G_{\alpha i}$ inhibitor; C and D) had no effect on U-50,488-induced translocation of PKCδ-eGFP (n = 3–4 cells per experiment; *p < 0.05; Student's paired t test in B; one-way ANOVA followed by Dunnett's multiple comparison test).

(E and F) Western blots (E) and quantified data (F) showing that U-50,488-induced GRPR phosphorylation is blocked by U73122, but not U73343. Data are represented as mean ± SEM. See also Figure S5.

(G) Schematic showing signaling events by which KOR activation results in GRPR desensitization. KOR activation by U-50,488 stimulates PLC to hydrolyze PIP_2 into DAG, which in turn induces PKCδ translocation from the cytosol to the plasma membrane, resulting in GRPR phosphorylation and desensitization.

(H) Schematic illustrates concurrent activation of two distinct subpopulations of dorsal horn interneurons by U-50,488: activation of KOR neurons without GRPR mediates anti-nociceptive output, whereas activation of KOR/GRPR neurons inhibits itch.

by which GRPR is phosphorylated and desensitized. Importantly, behavioral studies indicate that PKCδ-mediated desensitization of GRPR is long lasting. Previous *in vitro* studies suggested that the classic GRPR-PLC-IP_3 Ca^{2+} signaling activates kinases other than PKC (Kroog et al., 1995), and GRPR agonist-induced Ca^{2+}-dependent desensitization is transient and lasts less than 2 min (Zhao et al., 2014a). It is possible that distinct phosphorylation sites at the C-terminal domain of GRPR may contribute to the duration of desensitization (Ally et al., 2003). Whether PKCδ desensitizes agonist-unoccupied GRPR via direct phosphorylation or indirectly via other kinases awaits further studies (Kelly et al., 2008). Direct examination of spinal GRPR phosphorylation levels after KOR activation requires an antibody that can specifically detect phosphorylated GRPR *in vivo*, which contains multiple potential phosphorylation sites on its C terminus (Ally et al., 2003). Several lines of evidence fail to support the view that the endogenous dynorphin is an important modulator of itch transmission (Kardon et al., 2014): first, consistent with previous studies using either *Pdyn* KO mice or ablation of spinal Dyn^+ neurons (Duan et al., 2014; Kardon et al., 2014), *Pdyn* KO mice showed normal acute and chronic itch behaviors. Second, KOR agonists attenuate GRPR function via a long-lasting phosphorylation rather than acute desensitization process, the former of which rarely occurs under normal physiological condition. These observations are in support of the notion that KOR-GRPR cross-signaling induced by exogenous KOR agonists reflects an artificial process. While there is no evidence that the endogenous dynorphin modulates itch in normal physiological context, the possibility that a dramatic down-regulation of *Pdyn* in chronic itch condition (data not shown) may suggest an attenuation of inhibitory circuit cannot be excluded.

In summary, we demonstrate a non-canonical opioid signaling mechanism by which GRPR activity is attenuated by KOR-mediated cross-signaling in the spinal cord of mice. The finding of the inhibitory effect of KOR activation and its downstream signaling components on distinct types of chronic itch ($BRAF^{Nav1.8}$, ACD, and AEW) suggests a possibility for a broader application of KOR-GRPR-based anti-itch strategy to the treatment of chronic itch with various etiologies.

EXPERIMENTAL PROCEDURES

Animals

Behavioral tests were carried out on C57BL/6J, *Oprk1*$^{-/-}$ (Hough et al., 2000), *Grpr* KO (Hampton et al., 1998), BRAF$^{Nav1.8}$ (Zhao et al., 2013), *Grpr*^{iCre}, Ai9 (MMRRC), *Arrb2*$^{-/-}$ (Bohn et al., 1999), and *Prkcd*$^{-/-}$ (Leitges et al., 2001) male mice and their WT littermates unless indicated otherwise. All experiments conform to guidelines set by the NIH and the International Association for the Study of Pain and were reviewed and approved by the Animal Studies Committee at Washington University School of Medicine.

Itch Behavior

Mice were individually put into observation boxes and videotaped. The videos were played back on a computer and quantified by an observer who was blinded to the treatment or mice genotype. A scratch is defined as a bout of scratching that occurs after the mouse lifts its hind paw to the moment the hind paw is returned to the ground or mouth (Sun and Chen, 2007). For the dry-skin model, mice were painted twice daily with a mixture of acetone and diethyl ether (1:1) followed by water. Scratching behavior directed at the neck was counted in the morning before treatment (Miyamoto et al., 2002; Zhao et al., 2013). For ACD model, mice were sensitized by applying 100 μL of 0.15% DNFB on abdominal skin. One week later, mice were challenged by nape application of 50 μL of 0.15% DNFB every 2 or 3 days. Scratching responses were measured 24 hr after applying DNFB (Zhao et al., 2013).

RNAscope *In Situ* Hybridization and Immunohistochemistry

RNAscope ISH and IHC staining were performed as described (Wang et al., 2012; Zhao et al., 2014a). Spinal sections were processed according to the manufacturer's instructions in the RNAscope Fluorescent Multiplex Assay v2 manual for fixed frozen tissue (Advanced Cell Diagnostics).

siRNA Studies

Prkcd siRNA (Sigma) was delivered to the lumbar region of the spinal cord via i.t. injection as described (Liu et al., 2011; Zhao et al., 2014a). Mice were injected twice daily for 3 consecutive days, and behavior was performed 24 hr after the last injection.

Dissociation of Dorsal Horn Neurons and Calcium Imaging

Primary culture of spinal dorsal horn neurons was prepared from 5- to 7-day-old C57BL/6J mice and seeded onto 12-mm coverslips coated with poly-D-lysine. Calcium imaging was performed 3–5 days after seeding as described previously (Zhao et al., 2014a).

Whole-Cell Phosphorylation Assay

HEK293 cells expressing FLAG-KOR and Myc-GRPR were incubated in 10 μM U-50,488 or 1 μM PMA at 37°C and lysed as described (Liu et al., 2011). Proteins were incubated with mouse anti-Myc antibody (Sigma) overnight. The complex was precipitated, resolved on polyacrylamide gels, and transferred to polyvinylidene fluoride (PVDF) membranes (Millipore). Proteins were detected by immunoblotting with mouse anti-phosphoserine antibody (1:2,500; Sigma) overnight, and the blot was developed by enhanced chemiluminescence (Thermo Scientific).

PKC Translocation Assay

KOR-GRPR HEK293 cells, transiently expressing PKCδ-EGFP or PKCα-EGFP (kindly provided by Dr. Peter M. Blumbergtaken) were seeded in 29-mm glass bottom dishes (*In Vitro* Scientific). After 24 hr, the subcellular distribution of EGFP-fused protein was analyzed on a Leica TCS SPE confocal microscope.

Statistical Analysis

Statistical comparisons were performed with Graphpad Prism 7. Groups were considered significantly different if $p < 0.05$. Results are presented as the mean ± SEM.

SUPPLEMENTAL INFORMATION

Supplemental Information includes Supplemental Experimental Procedures, seven figures, two tables, and four videos and can be found with this article online at https://doi.org/10.1016/j.celrep.2018.03.087.

ACKNOWLEDGMENTS

We thank the Chen laboratory for comments. D.M.B. was supported by W.M. Keck Fellowship and NIH-NIDA T32 Training Grant (5T32DA007261-23). The project was supported by NIAMS AR056318-06 (Z.-F.C.), NINDS NS094344 (Z.-F.C.), NIDA RO1DA037261-01A1 (Z.-F.C.), The National Natural Science Foundation of China (grants 31371211 and 81620108008) (H.L. and Y.-Q.L.), and DA033396 (M.R.B.).

AUTHOR CONTRIBUTIONS

Conceptualization, Z.-F.C.; Investigation, A.M., X.-Y.L., D.M.B., Q.Y., J.-B.Y., H.J., Q.-T.M., J.-H.P., Z.-Y.W., J.Y., X.-Y.Z., L.W., P.M., S.K., F.-Q.H., J.J., and R.B.; Resources, J.Y.; Writing – Original Draft, A.M., X.-Y.L., and Z.-F.C.; Formal Analysis, A.M. and X.-Y.L.; Writing – Review & Editing, Z.-F.C., A.M., X.-Y.L., D.M.B., and M.R.B.; Funding Acquisition, Z.-F.C., H.L., Y.-Q.L., and M.R.B.; Supervision, Z.-F.C.

DECLARATION OF INTERESTS

The authors declare no competing interests.

Received: December 5, 2017
Revised: February 28, 2018
Accepted: March 20, 2018
Published: April 17, 2018

REFERENCES

Abeliovich, A., Chen, C., Goda, Y., Silva, A.J., Stevens, C.F., and Tonegawa, S. (1993). Modified hippocampal long-term potentiation in PKC gamma-mutant mice. Cell *75*, 1253–1262.

Ajayi, A.A., Oluokun, A., Sofowora, O., Akinleye, A., and Ajayi, A.T. (1989). Epidemiology of antimalarial-induced pruritus in Africans. Eur. J. Clin. Pharmacol. *37*, 539–540.

Akiyama, T., Tominaga, M., Davoodi, A., Nagamine, M., Blansit, K., Horwitz, A., Carstens, M.I., and Carstens, E. (2013). Roles for substance P and gastrin-releasing peptide as neurotransmitters released by primary afferent pruriceptors. J. Neurophysiol. *109*, 742–748.

Akiyama, T., Tominaga, M., Takamori, K., Carstens, M.I., and Carstens, E. (2014). Roles of glutamate, substance P, and gastrin-releasing peptide as spinal neurotransmitters of histaminergic and nonhistaminergic itch. Pain *155*, 80–92.

Al-Hasani, R., and Bruchas, M.R. (2011). Molecular mechanisms of opioid receptor-dependent signaling and behavior. Anesthesiology *115*, 1363–1381.

Ally, R.A., Ives, K.L., Traube, E., Eltounsi, I., Chen, P.W., Cahill, P.J., Battey, J.F., Hellmich, M.R., and Kroog, G.S. (2003). Agonist- and protein kinase C-induced phosphorylation have similar functional consequences for gastrin-releasing peptide receptor signaling via Gq. Mol. Pharmacol. *64*, 890–904.

Ballantyne, J.C., Loach, A.B., and Carr, D.B. (1988). Itching after epidural and spinal opiates. Pain *33*, 149–160.

Barry, D.M., Li, H., Liu, X.Y., Shen, K.F., Liu, X.T., Wu, Z.Y., Munanairi, A., Chen, X.J., Yin, J., Sun, Y.G., et al. (2016). Critical evaluation of the expression of gastrin-releasing peptide in dorsal root ganglia and spinal cord. Mol. Pain *12*, 1744806916643724.

Barry, D.M., Munanairi, A., and Chen, Z.F. (2018). Spinal mechanisms of itch transmission. Neurosci. Bull. *34*, 156–164.

Bautista, D.M., Wilson, S.R., and Hoon, M.A. (2014). Why we scratch an itch: the molecules, cells and circuits of itch. Nat. Neurosci. *17*, 175–182.

Bigliardi-Qi, M., Gaveriaux-Ruff, C., Pfaltz, K., Bady, P., Baumann, T., Rufli, T., Kieffer, B.L., and Bigliardi, P.L. (2007). Deletion of mu- and kappa-opioid receptors in mice changes epidermal hypertrophy, density of peripheral nerve endings, and itch behavior. J. Invest. Dermatol. *127*, 1479–1488.

Bohn, L.M., Lefkowitz, R.J., Gainetdinov, R.R., Peppel, K., Caron, M.G., and Lin, F.T. (1999). Enhanced morphine analgesia in mice lacking beta-arrestin 2. Science *286*, 2495–2498.

Bohn, L.M., Belcheva, M.M., and Coscia, C.J. (2000). Mitogenic signaling via endogenous kappa-opioid receptors in C6 glioma cells: evidence for the involvement of protein kinase C and the mitogen-activated protein kinase signaling cascade. J. Neurochem. *74*, 564–573.

Bruchas, M.R., and Chavkin, C. (2010). Kinase cascades and ligand-directed signaling at the kappa opioid receptor. Psychopharmacology (Berl.) *210*, 137–147.

Chakrabarti, S., Liu, N.J., and Gintzler, A.R. (2010). Formation of mu-/kappa-opioid receptor heterodimer is sex-dependent and mediates female-specific opioid analgesia. Proc. Natl. Acad. Sci. USA *107*, 20115–20119.

Chavkin, C., James, I.F., and Goldstein, A. (1982). Dynorphin is a specific endogenous ligand of the kappa opioid receptor. Science *215*, 413–415.

Choi, E.B., Chen, Z.-F., Zhu, Z., and Zheng, T. (2016). The role of gastrin releasing peptide (GRP) in atopic dermatitis (AD) induced by interleukin 13 (IL-13). J. Allergy Clin. Immunol. *137*, AB182.

Chuang, L.F., Chuang, T.K., Killam, K.F., Jr., Qiu, Q., Wang, X.R., Lin, J.J., Kung, H.F., Sheng, W., Chao, C., Yu, L., et al. (1995). Expression of kappa opioid receptors in human and monkey lymphocytes. Biochem. Biophys. Res. Commun. *209*, 1003–1010.

Cowan, A., Kehner, G.B., and Inan, S. (2015). Targeting itch with ligands selective for κ opioid receptors. Handb. Exp. Pharmacol. *226*, 291–314.

Dawn, A.G., and Yosipovitch, G. (2006). Butorphanol for treatment of intractable pruritus. J. Am. Acad. Dermatol. *54*, 527–531.

Duan, B., Cheng, L., Bourane, S., Britz, O., Padilla, C., Garcia-Campmany, L., Krashes, M., Knowlton, W., Velasquez, T., Ren, X., et al. (2014). Identification of spinal circuits transmitting and gating mechanical pain. Cell *159*, 1417–1432.

Dunteman, E., Karanikolas, M., and Filos, K.S. (1996). Transnasal butorphanol for the treatment of opioid-induced pruritus unresponsive to antihistamines. J. Pain Symptom Manage. *12*, 255–260.

Grudt, T.J., and Williams, J.T. (1993). kappa-opioid receptors also increase potassium conductance. Proc. Natl. Acad. Sci. USA *90*, 11429–11432.

Hampton, L.L., Ladenheim, E.E., Akeson, M., Way, J.M., Weber, H.C., Sutliff, V.E., Jensen, R.T., Wine, L.J., Arnheiter, H., and Battey, J.F. (1998). Loss of bombesin-induced feeding suppression in gastrin-releasing peptide receptor-deficient mice. Proc. Natl. Acad. Sci. USA *95*, 3188–3192.

Hough, L.B., Nalwalk, J.W., Chen, Y., Schuller, A., Zhu, Y., Zhang, J., Menge, W.M., Leurs, R., Timmerman, H., and Pintar, J.E. (2000). Improgan, a cimetidine analog, induces morphine-like antinociception in opioid receptor-knockout mice. Brain Res. *880*, 102–108.

Ikoma, A., Steinhoff, M., Ständer, S., Yosipovitch, G., and Schmelz, M. (2006). The neurobiology of itch. Nat. Rev. Neurosci. *7*, 535–547.

Inan, S., and Cowan, A. (2004). Kappa opioid agonists suppress chloroquine-induced scratching in mice. Eur. J. Pharmacol. *502*, 233–237.

Kagami, S., Sugaya, M., Suga, H., Morimura, S., Kai, H., Ohmatsu, H., Fujita, H., Tsunemi, Y., and Sato, S. (2013). Serum gastrin-releasing peptide levels correlate with pruritus in patients with atopic dermatitis. J. Invest. Dermatol. *133*, 1673–1675.

Kardon, A.P., Polgár, E., Hachisuka, J., Snyder, L.M., Cameron, D., Savage, S., Cai, X., Karnup, S., Fan, C.R., Hemenway, G.M., et al. (2014). Dynorphin acts as a neuromodulator to inhibit itch in the dorsal horn of the spinal cord. Neuron *82*, 573–586.

Kelly, E., Bailey, C.P., and Henderson, G. (2008). Agonist-selective mechanisms of GPCR desensitization. Br. J. Pharmacol. *153* (*Suppl 1*), S379–S388.

Ko, M.C., Lee, H., Song, M.S., Sobczyk-Kojiro, K., Mosberg, H.I., Kishioka, S., Woods, J.H., and Naughton, N.N. (2003). Activation of kappa-opioid receptors inhibits pruritus evoked by subcutaneous or intrathecal administration of morphine in monkeys. J. Pharmacol. Exp. Ther. *305*, 173–179.

Kroog, G.S., Jensen, R.T., and Battey, J.F. (1995). Mammalian bombesin receptors. Med. Res. Rev. *15*, 389–417.

Kumagai, H., Ebata, T., Takamori, K., Muramatsu, T., Nakamoto, H., and Suzuki, H. (2010). Effect of a novel kappa-receptor agonist, nalfurafine hydrochloride, on severe itch in 337 haemodialysis patients: a phase III, randomized, double-blind, placebo-controlled study. Nephrol. Dial. Transplant. *25*, 1251–1257.

Lagerström, M.C., Rogoz, K., Abrahamsen, B., Persson, E., Reinius, B., Nordenankar, K., Olund, C., Smith, C., Mendez, J.A., Chen, Z.F., et al. (2010). VGLUT2-dependent sensory neurons in the TRPV1 population regulate pain and itch. Neuron *68*, 529–542.

Land, B.B., Bruchas, M.R., Lemos, J.C., Xu, M., Melief, E.J., and Chavkin, C. (2008). The dysphoric component of stress is encoded by activation of the dynorphin kappa-opioid system. J. Neurosci. *28*, 407–414.

Lawhorn, C.D., McNitt, J.D., Fibuch, E.E., Joyce, J.T., and Leadley, R.J., Jr. (1991). Epidural morphine with butorphanol for postoperative analgesia after cesarean delivery. Anesth. Analg. *72*, 53–57.

Lee, H., and Ko, M.C. (2015). Distinct functions of opioid-related peptides and gastrin-releasing peptide in regulating itch and pain in the spinal cord of primates. Sci. Rep. *5*, 11676.

Leitges, M., Mayr, M., Braun, U., Mayr, U., Li, C., Pfister, G., Ghaffari-Tabrizi, N., Baier, G., Hu, Y., and Xu, Q. (2001). Exacerbated vein graft arteriosclerosis in protein kinase Cdelta-null mice. J. Clin. Invest. *108*, 1505–1512.

Liu, T., and Ji, R.-R. (2013). New insights into the mechanisms of itch: are pain and itch controlled by distinct mechanisms? Pflugers Arch. *465*, 1671–1685.

Liu, X.Y., Liu, Z.C., Sun, Y.G., Ross, M., Kim, S., Tsai, F.F., Li, Q.F., Jeffry, J., Kim, J.Y., Loh, H.H., and Chen, Z.F. (2011). Unidirectional cross-activation of GRPR by MOR1D uncouples itch and analgesia induced by opioids. Cell *147*, 447–458.

Lou, H., Lu, J., Choi, E.B., Oh, M.H., Jeong, M., Barmettler, S., Zhu, Z., and Zheng, T. (2017). Expression of IL-22 in the skin causes Th2-biased immunity, epidermal barrier dysfunction, and pruritus via stimulating epithelial Th2 cytokines and the GRP pathway. J. Immunol. *198*, 2543–2555.

Miyamoto, T., Nojima, H., Shinkado, T., Nakahashi, T., and Kuraishi, Y. (2002). Itch-associated response induced by experimental dry skin in mice. Jpn. J. Pharmacol. *88*, 285–292.

Mochly-Rosen, D., Henrich, C.J., Cheever, L., Khaner, H., and Simpson, P.C. (1990). A protein kinase C isozyme is translocated to cytoskeletal elements on activation. Cell Regul. *1*, 693–706.

Morgenweck, J., Frankowski, K.J., Prisinzano, T.E., Aubé, J., and Bohn, L.M. (2015). Investigation of the role of βarrestin2 in kappa opioid receptor modulation in a mouse model of pruritus. Neuropharmacology *99*, 600–609.

Nakazawa, T., Furuya, Y., Kaneko, T., and Yamatsu, K. (1990). Spinal kappa receptor-mediated analgesia of E-2078, a systematically active dynorphin analogue. Eur. J. Pharmacol. *183*, 2329.

Nattkemper, L.A., Zhao, Z.Q., Nichols, A.J., Papoiu, A.D.P., Shively, C.A., Chen, Z.F., and Yosipovitch, G. (2013). Overexpression of the gastrin-releasing peptide in cutaneous nerve fibers and its receptor in the spinal cord in primates with chronic itch. J. Invest. Dermatol. *133*, 2489–2492.

Nishizuka, Y. (1995). Protein kinase C and lipid signaling for sustained cellular responses. FASEB J. *9*, 484–496.

Oancea, E., Teruel, M.N., Quest, A.F., and Meyer, T. (1998). Green fluorescent protein (GFP)-tagged cysteine-rich domains from protein kinase C as fluorescent indicators for diacylglycerol signaling in living cells. J. Cell Biol. *140*, 485–498.

Pan, Z.Z. (1998). mu-opposing actions of the kappa-opioid receptor. Trends Pharmacol. Sci. *19*, 94–98.

Paus, R., Schmelz, M., Bíró, T., and Steinhoff, M. (2006). Frontiers in pruritus research: scratching the brain for more effective itch therapy. J. Clin. Invest. *116*, 1174–1186.

Phan, N.Q., Lotts, T., Antal, A., Bernhard, J.D., and Ständer, S. (2012). Systemic kappa opioid receptor agonists in the treatment of chronic pruritus: a literature review. Acta Derm. Venereol. *92*, 555–560.

Porreca, F., Mosberg, H.I., Hurst, R., Hruby, V.J., and Burks, T.F. (1984). Roles of mu, delta and kappa opioid receptors in spinal and supraspinal mediation of gastrointestinal transit effects and hot-plate analgesia in the mouse. J. Pharmacol. Exp. Ther. *230*, 341–348.

Portoghese, P.S., Lipkowski, A.W., and Takemori, A.E. (1987). Binaltorphimine and nor-binaltorphimine, potent and selective kappa-opioid receptor antagonists. Life Sci. *40*, 1287–1292.

Randić, M., Cheng, G., and Kojic, L. (1995). kappa-opioid receptor agonists modulate excitatory transmission in substantia gelatinosa neurons of the rat spinal cord. J. Neurosci. *15*, 6809–6826.

Reich, A., and Szepietowski, J.C. (2010). Opioid-induced pruritus: an update. Clin. Exp. Dermatol. *35*, 2–6.

Sakakihara, M., Imamachi, N., and Saito, Y. (2016). Effects of intrathecal κ-opioid receptor agonist on morphine-induced itch and antinociception in mice. Reg. Anesth. Pain Med. *41*, 69–74.

Shiratori-Hayashi, M., Koga, K., Tozaki-Saitoh, H., Kohro, Y., Toyonaga, H., Yamaguchi, C., Hasegawa, A., Nakahara, T., Hachisuka, J., Akira, S., et al. (2015). STAT3-dependent reactive astrogliosis in the spinal dorsal horn underlies chronic itch. Nat. Med. *21*, 927–931.

Simonin, F., Valverde, O., Smadja, C., Slowe, S., Kitchen, I., Dierich, A., Le Meur, M., Roques, B.P., Maldonado, R., and Kieffer, B.L. (1998). Disruption of the kappa-opioid receptor gene in mice enhances sensitivity to chemical visceral pain, impairs pharmacological actions of the selective kappa-agonist U-50,488H and attenuates morphine withdrawal. EMBO J. *17*, 886–897.

Steinberg, S.F. (2008). Structural basis of protein kinase C isoform function. Physiol. Rev. *88*, 1341–1378.

Sun, Y.G., and Chen, Z.F. (2007). A gastrin-releasing peptide receptor mediates the itch sensation in the spinal cord. Nature *448*, 700–703.

Sun, Y.G., Zhao, Z.Q., Meng, X.L., Yin, J., Liu, X.Y., and Chen, Z.F. (2009). Cellular basis of itch sensation. Science *325*, 1531–1534.

Suzuki, S., Chuang, L.F., Doi, R.H., Bidlack, J.M., and Chuang, R.Y. (2001). Kappa-opioid receptors on lymphocytes of a human lymphocytic cell line: morphine-induced up-regulation as evidenced by competitive RT-PCR and indirect immunofluorescence. Int. Immunopharmacol. *1*, 1733–1742.

Takanami, K., Sakamoto, H., Matsuda, K.I., Satoh, K., Tanida, T., Yamada, S., Inoue, K., Oti, T., Sakamoto, T., and Kawata, M. (2014). Distribution of gastrin-releasing peptide in the rat trigeminal and spinal somatosensory systems. J. Comp. Neurol. *522*, 1858–1873.

Tirado-Sánchez, A., Bonifaz, A., and Ponce-Olivera, R.M. (2015). Serum gastrin-releasing peptide levels correlate with disease severity and pruritus in patients with atopic dermatitis. Br. J. Dermatol. *173*, 298–300.

Togashi, Y., Umeuchi, H., Okano, K., Ando, N., Yoshizawa, Y., Honda, T., Kawamura, K., Endoh, T., Utsumi, J., Kamei, J., et al. (2002). Antipruritic activity of the kappa-opioid receptor agonist, TRK-820. Eur. J. Pharmacol. *435*, 259–264.

Tominaga, M., Ogawa, H., and Takamori, K. (2009). Histological characterization of cutaneous nerve fibers containing gastrin-releasing peptide in NC/Nga mice: an atopic dermatitis model. J. Invest. Dermatol. *129*, 2901–2905.

Toullec, D., Pianetti, P., Coste, H., Bellevergue, P., Grand-Perret, T., Ajakane, M., Baudet, V., Boissin, P., Boursier, E., Loriolle, F., et al. (1991). The bisindolylmaleimide GF 109203X is a potent and selective inhibitor of protein kinase C. J. Biol. Chem. *266*, 15771–15781.

Wan, L., Jin, H., Liu, X.Y., Jeffry, J., Barry, D.M., Shen, K.F., Peng, J.H., Liu, X.T., Jin, J.H., Sun, Y., et al. (2017). Distinct roles of NMB and GRP in itch transmission. Sci. Rep. *7*, 15466.

Wang, Q.J., Bhattacharyya, D., Garfield, S., Nacro, K., Marquez, V.E., and Blumberg, P.M. (1999). Differential localization of protein kinase C delta by phorbol esters and related compounds using a fusion protein with green fluorescent protein. J. Biol. Chem. *274*, 37233–37239.

Wang, F., Flanagan, J., Su, N., Wang, L.C., Bui, S., Nielson, A., Wu, X., Vo, H.T., Ma, X.J., and Luo, Y. (2012). RNAscope: a novel in situ RNA analysis platform for formalin-fixed, paraffin-embedded tissues. J. Mol. Diagn. *14*, 22–29.

Wang, X., Zhang, J., Eberhart, D., Urban, R., Meda, K., Solorzano, C., Yamanaka, H., Rice, D., and Basbaum, A.I. (2013). Excitatory superficial dorsal horn interneurons are functionally heterogeneous and required for the full behavioral expression of pain and itch. Neuron *78*, 312–324.

Way, K.J., Chou, E., and King, G.L. (2000). Identification of PKC-isoform-specific biological actions using pharmacological approaches. Trends Pharmacol. Sci. *21*, 181–187.

Wikström, B., Gellert, R., Ladefoged, S.D., Danda, Y., Akai, M., Ide, K., Ogasawara, M., Kawashima, Y., Ueno, K., Mori, A., and Ueno, Y. (2005). Kappa-opioid system in uremic pruritus: multicenter, randomized, double-blind, placebo-controlled clinical studies. J. Am. Soc. Nephrol. *16*, 3742–3747.

Xu, M., Petraschka, M., McLaughlin, J.P., Westenbroek, R.E., Caron, M.G., Lefkowitz, R.J., Czyzyk, T.A., Pintar, J.E., Terman, G.W., and Chavkin, C. (2004). Neuropathic pain activates the endogenous kappa opioid system in mouse spinal cord and induces opioid receptor tolerance. J. Neurosci. *24*, 4576–4584.

Zhao, Z.Q., Huo, F.Q., Jeffry, J., Hampton, L., Demehri, S., Kim, S., Liu, X.Y., Barry, D.M., Wan, L., Liu, Z.C., et al. (2013). Chronic itch development in sensory neurons requires BRAF signaling pathways. J. Clin. Invest. *123*, 4769–4780.

Zhao, Z.Q., Liu, X.Y., Jeffry, J., Karunarathne, W.K., Li, J.L., Munanairi, A., Zhou, X.Y., Li, H., Sun, Y.G., Wan, L., et al. (2014a). Descending control of itch transmission by the serotonergic system via 5-HT1A-facilitated GRP-GRPR signaling. Neuron *84*, 821–834.

Zhao, Z.Q., Wan, L., Liu, X.Y., Huo, F.Q., Li, H., Barry, D.M., Krieger, S., Kim, S., Liu, Z.C., Xu, J., et al. (2014b). Cross-inhibition of NMBR and GRPR signaling maintains normal histaminergic itch transmission. J. Neurosci. *34*, 12402–12414.

Cell Reports, Volume *23*

Supplemental Information

Non-canonical Opioid Signaling Inhibits Itch Transmission in the Spinal Cord of Mice

Admire Munanairi, Xian-Yu Liu, Devin M. Barry, Qianyi Yang, Jun-Bin Yin, Hua Jin, Hui Li, Qing-Tao Meng, Jia-Hang Peng, Zhen-Yu Wu, Jun Yin, Xuan-Yi Zhou, Li Wan, Ping Mo, Seungil Kim, Fu-Quan Huo, Joseph Jeffry, Yun-Qing Li, Rita Bardoni, Michael R. Bruchas, and Zhou-Feng Chen

Supplemental Information

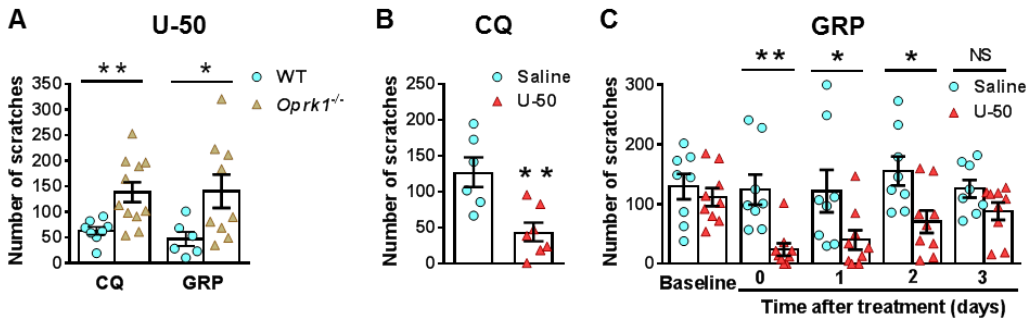

Figure S1. Intrathecal U-50,488 Inhibition of Itch is Long-lasting. Related to Figure 1

(A) U-50,488 lost its inhibitory effect on scratching induced by GRP and CQ in *Oprk1*$^{-/-}$ mice (*p < 0.05, **p < 0.01, Student's unpaired t test, n = 6–11).

(B) U-50,488 significantly reduced scratching induced by CQ in female mice (**p < 0.01, Student's unpaired t test, n = 6–7).

(C) GIS is unchanged after multiple injections. U-50,488 inhibition of GRP-induced scratching lasts 48 h. (*p < 0.05, **p < 0.01, two way ANOVA followed by Bonferroni posttest, n = 8).

Data are represented as mean ± SEM.

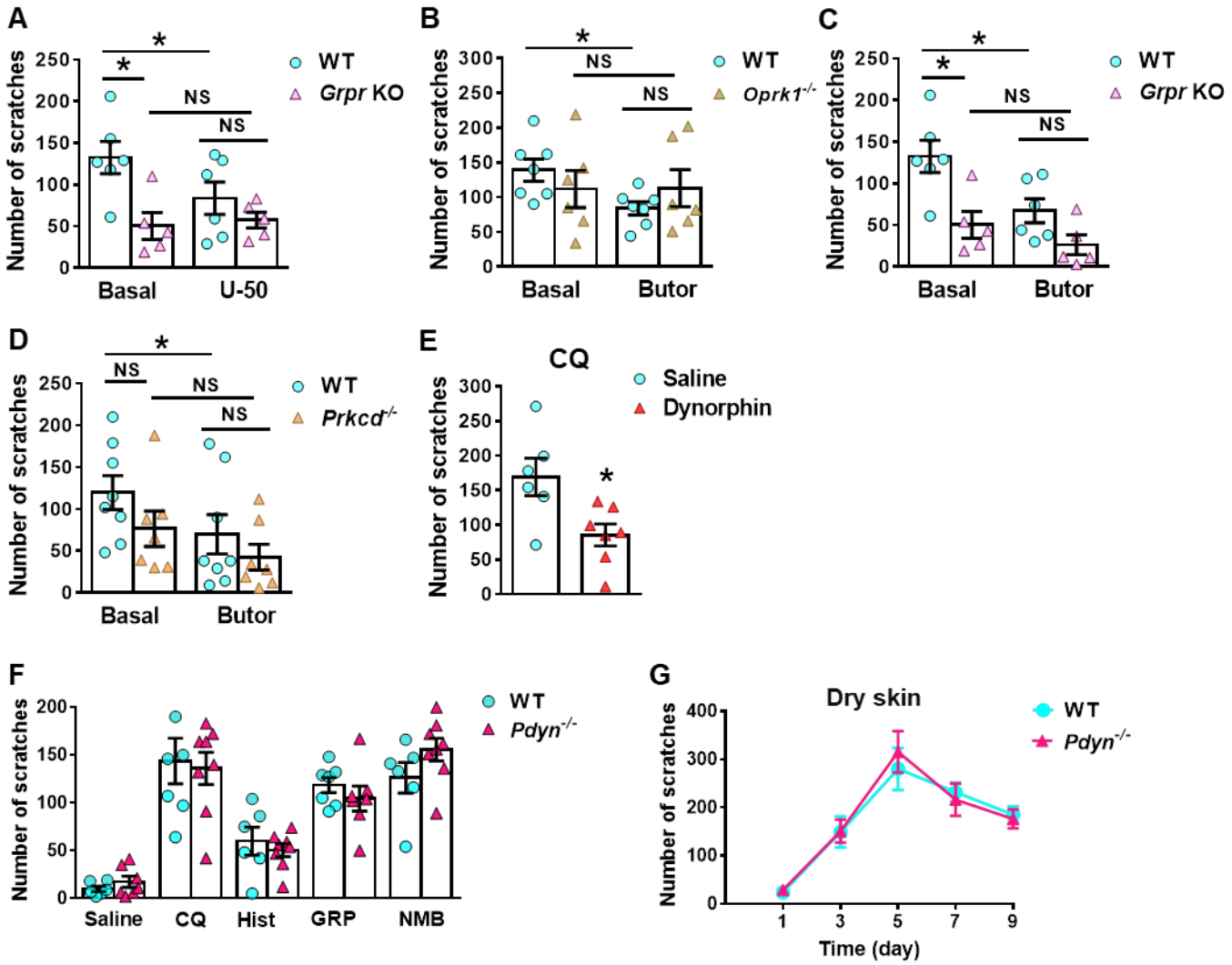

Figure S2. Spinal KOR Activation Inhibition of Itch Is Mediated by Cell Autonomous Effects. Related to Figures 1 and 2

(A) I.t. U-50,488 lost its inhibitory effect on scratching induced by CQ in *Grpr* KO mice (*p < 0.05, NS, not significant, Student's unpaired t test or paired t test, (basal relative to U-50), n = 5–6).

(B) I.t. butorphanol (2 nmol) significantly reduced scratching induced by CQ in WT but not *Oprk1*$^{-/-}$ littermates (*p < 0.05, Student's paired t test, n = 6–7).

(C) I.t. butorphanol loses inhibitory effects on scratching induced by CQ in *Grpr* KO mice (*p < 0.05, NS, not significant, Student's unpaired t test or paired t test, (basal relative to Butor), n = 5–6).

(D) Butorphanol (2 nmol) significantly reduced scratching induced by CQ in WT but not *Prkcd*$^{-/-}$ littermates (*p < 0.05, Student's unpaired t test or paired t test, (basal relative to Butor), n = 7–8).

(E) Dynorphin significantly reduced scratching induced by CQ (*p < 0.05, Student's unpaired t test, n = 6-7). Data are represented as mean ± SEM.

(F) WT littermate controls and *Pdyn*$^{-/-}$ mice exhibited no difference in scratching induced by CQ, Hist, GRP and NMB (n = 6–8).

(G) Dry skin itch was comparable in *Pdyn*$^{-/-}$ mice and WT (n = 9–14).

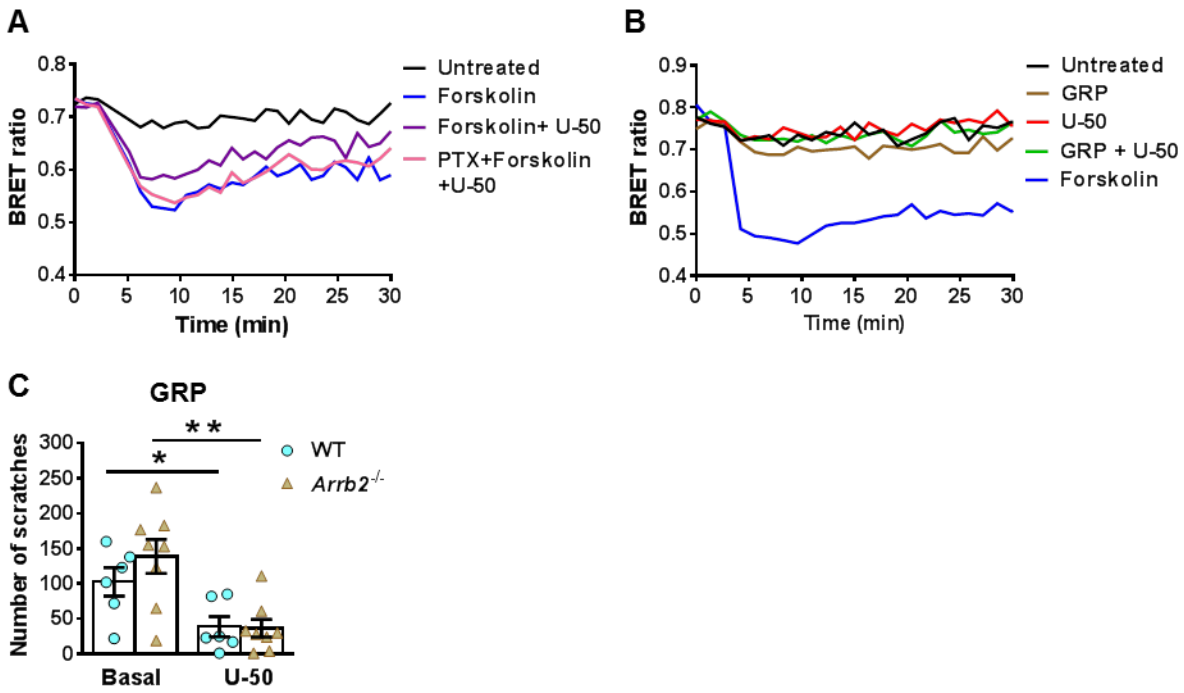

Figure S3. KOR Activation Suppresses GRPR Activity in $G_{\alpha s}$- and β-arrestin2-independent Manner. Related to Figure 2

(A) BRET assay showing that U-50,488 (10 μM) attenuated forskolin-induced increase in cAMP levels (purple). PTX (200 ng/ml) reversed the effect of U-50,488 (pink). RLuc-EPAC-Venus (1.0 μg) was used as a BRET sensor. Blank media was used as a control (black).

(B) 1 μM GRP or 10 μM U-50,488 or a co-incubation of U-50,488 and GRP does not induce an increase in cAMP levels (brown, red and green traces respectively).

(C) *Arrb2*$^{-/-}$ and their WT littermates mice exhibited no difference in scratching induced by GRP. I.t. U-50,488 attenuated scratching induced by GRP in both *Arrb2*$^{-/-}$ and their WT littermates (*$p < 0.05$, **$p < 0.01$, Student's unpaired t test or paired t test, basal relative to U-50), n = 6–8).

Data are represented as mean ± SEM.

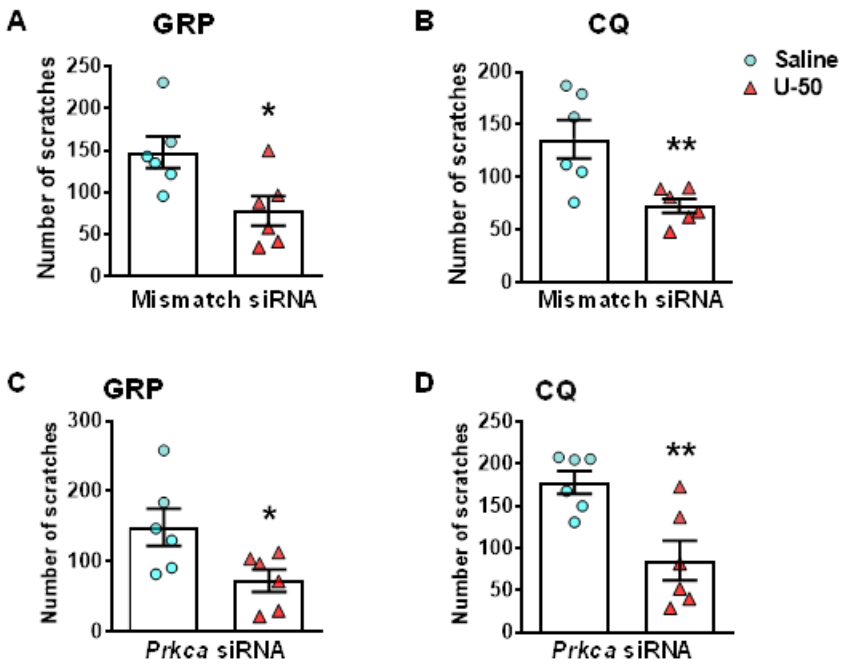

Figure S4. U-50,488 Inhibits Itch After Treatment of *Prkcd* Mismatch Control siRNA and *Prkca* siRNA. Related to Figure 5

(A) U-50,488 attenuated scratching induced by GRP (0.3 nmol) in control siRNA-treated mice (*$p < 0.05$, unpaired t test, n = 6).

(B) U-50,488 attenuated scratching induced by CQ (200 µg) in control siRNA-treated mice (**$p < 0.01$, unpaired t test, n = 6).

(C) U-50,488 attenuated scratching induced by GRP (0.3 nmol) in *Prkca* siRNA-treated mice (*$p < 0.05$, unpaired t test, n = 6).

(D) U-50,488 attenuated scratching induced by CQ (200 µg) in *Prkca* siRNA-treated mice (**$p < 0.01$, unpaired t test test, n = 6).

Data are represented as mean ± SEM.

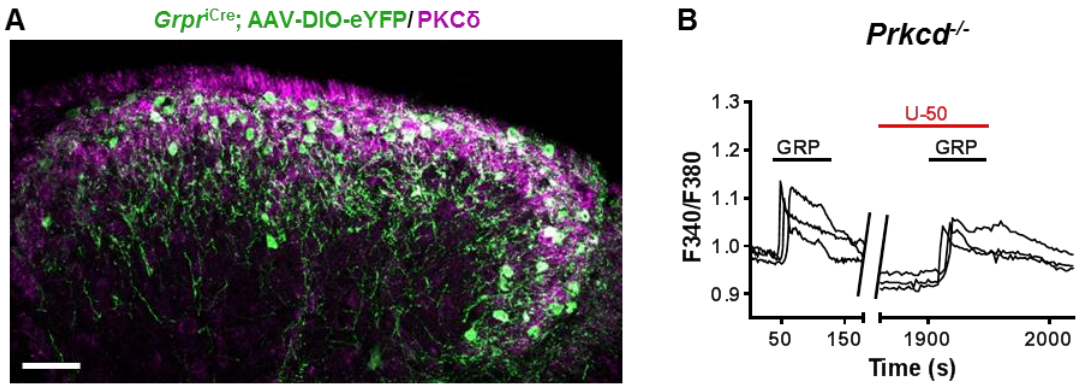

Figure S5. Expression of PKCδ in GRPR Neurons. Related to Figure 5

(A) Double IHC of PKCδ (purple) and eYFP (green) shows co-expression of GRPR and PKCδ in superficial dorsal horn neurons of *Grpr*^{iCre} mice injected with AAV-DIO-eYFP. Scale bar, 50 μm.

(B) Representative traces showing U-50,488 had no effect on inhibited GRP-induced Ca^{2+} responses in dissociated dorsal horn neurons from *Prkcd*$^{-/-}$ mice.

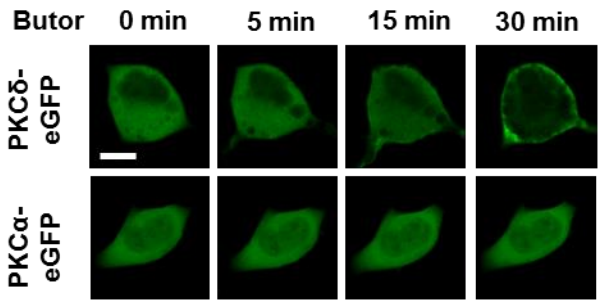

Figure S6. Butorphanol Induces Translocation of PKCδ but not PKCα to the Plasma Membrane. Related to Figure 6

HEK293 cells expressing KOR/GRPR transfected with PKCδ-eGFP (upper row) and PKCα-eGFP (lower row) were incubated in 20 μM butorphanol. Confocal images taken at indicated time points showed that butorphanol induced the translocation of PKCδ-eGFP but not PKCα-eGFP to the plasma membrane (scale bar, 20 μm).

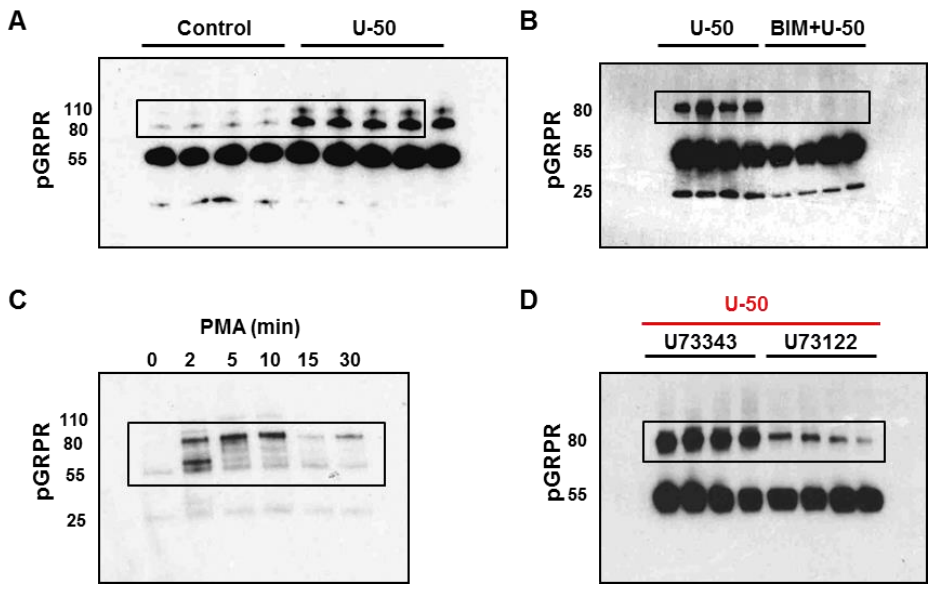

Figure S7. Related to Figures 4 and 7. (A-D) Full size unedited gels for phosphorylated GRPR (pGRPR) for Figures 4A, 4C, 4D and 7E respectively. The boxed regions correspond to those shown in the cropped images within the respective figures. The numbers represent molecular weight of the respective bands (in kDa).

Supplemental Tables

Table S1. Characterization of GRP-induced calcium responses of GRPR neurons (control). **Related to Figure 2**

Cell type (normalized to first GRP response)	**Fractional Responses to GRP**
Non-responders (0-10 %)	2/32 (6 %)
Reduction (10-50 %)	3/32 (9 %)
Responders (> 50 %)	27/32 (84 %)

Table S2. Characterization of GRP-induced calcium responses of GRPR neurons after U-50,488 treatment. **Related to Figure 2**

Cell type (normalized to first GRP response)	**Fractional Responses to GRP**
Non-responders (0-10 %)	52/124 (42 %)
Reduction (10-50 %)	32/124 (26 %)
Responders (> 50 %)	40/124 (32 %)

Supplemental Experimental Procedures

Animals

All behavioral experiments conform to guidelines set by the National Institute of Health and the International Association for the Study of Pain, and were reviewed and approved by the Animal Studies Committee at Washington University School of Medicine**.** Mice were housed in a controlled environment with free access to food and water. The animal room was on a 12/12 h light/dark cycle with lights on at 0700 h. C57BL/6J, *Oprk1*$^{-/-}$ (Hough et al., 2000), *Grpr* KO(Hampton et al., 1998), BRAF$^{Nav1.8}$ (Zhao et al., 2013), *Grpr*^{iCre} (its generation will be described in a separate manuscript), Ai9 (MMRRC), *Arrb2*$^{-/-}$ (Bohn et al., 1999), *Prkcd*$^{-/-}$ (Leitges et al., 2001), *Pdyn*$^{-/-}$ (Sharifi et al., 2001), and their WT littermates were used for this study. Male mice were used for all experiments, except Figure S1B.

Drugs and Reagents

Drugs were from Sigma, unless otherwise indicated. U-50,488, butorphanol (Zoetis), GRP, NMB (Bachem), CQ, histamine, BIM, PMA, norBNI, PTX (Tocris) were dissolved in sterile 0.9 % saline. Forskolin, gallein, U73122 and U73343 were from Tocris and dissolved in DMSO. Other relevant information is included in results and figure legends.

Itch Behavior

Acute Itch

Behavioral experiments were performed during the day (0800 – 1500 h). For i.t. injections, mice had their backs shaved off a day before the experiments. On the test day, mice were given at least 30 min to get accustomed to recording conditions prior to injections and recordings. For i.t. injections, a 30-gauge needle was inserted into the intervertebral space between L5 and L6. Drugs were injected in a volume of 5 μI. I.t. placement was confirmed by a swift flick of the tail on needle entry. Immediately after injections, mice were put into rectangular, transparent observation boxes (10 × 11 × 15 cm) and videotaped using SONY HDR-CX190 digital video camcorders from a side angle. The videos were played back on a computer and quantified by an observer who was blinded to the treatment or mice genotype. For time-course analysis, scratches were recorded every 5 min immediately after injection. A scratch is defined as a bout of scratching that occurs after the mouse lifts its hind-paw to the moment the hind-paw is returned to the ground, mouth or paused (a bout usually lasts about 5 seconds). Each mouse was observed for 30 minutes, and the number of scratches recorded. For intradermal injections, briefly mice had a small part of their necks shaved, and 50 μl of the test substance was injected using a syringe attached to a SS30M3009 – 3/10 cc, 30G × 3/8" needle (Terumo). Only scratches to the injection site were counted for 30 min. These behavioral studies are based on an already published protocol (Sun and Chen, 2007).

Chronic Itch Mouse Models

Dry Skin (AEW) Model: Mice were treated with an acetone/ether mixture followed by water, inducing spontaneous scratching. Briefly, cotton socked with a mixture of acetone and diethyl ether (1:1) was applied on the nape of the neck for 15 s, followed by 30 s of cotton soaked in water. This procedure was performed twice daily for

9 days, with a 6 h window in-between. Scratching behavior directed at the neck was counted for 1 h the morning before treatment by an observer who was blinded to the treatment (Miyamoto et al., 2002; Zhao et al., 2013).

BRAF$^{Nav1.8}$ Mice: BRAF$^{Nav1.8}$ mice, at least 6 weeks old, which would have developed spontaneous scratching and their WT littermates were used in this study (Zhao et al., 2013).

ACD Model: C57BL/6J male mice were sensitized by applying 100 µl of 0.15 % DNFB acetone solution on ~2 cm^2 area of fur-shaved abdominal skin (sensitization, day 1). On day 8, 50 µl of 0.15% DNFB acetone solution was topically applied twice a week (every 2-3 days) to the clipped rostral part of mouse back for over 3 weeks (challenge). Scratching responses were measured 24 h after applying DNFB by an observer who was blinded to the treatment (Zhao et al., 2013).

Small Interfering RNA Treatment

Negative control siRNA (SC001) and selective duplex siRNA for mouse *Prkcd* mRNA (SASI_Mm02_00319898), *Prkca* mRNA (SASI_Mm02_00162578), and mismatch control siRNA for mouse *Prkcd* mRNA were purchased from Sigma. RNA was dissolved in diethyl pyrocarbonate-treated PBS and prepared immediately prior to administration by mixing the RNA solution with a transfection reagent, in vivo-jet PEI®(Polyplus-transfection SA). The final concentration of RNA was 1.25 µg/10 µl. siRNA was delivered to the lumbar region of the spinal cord. Mice were injected twice daily for 3 consecutive days as described previously (Liu et al., 2011; Liu et al., 2014; Zhao et al., 2014b). Behavioral testing was carried out 24 h after the last injection. The spinal cord tissue was collected for RT-PCR after 1 more day of siRNA injections.

RNAscope *In Situ* Hybridization (ISH)

RNAscope ISH was performed as described (Wang et al., 2012). Briefly, mice were anesthetized with a ketamine/xylazine cocktail (ketamine, 100 mg/kg and xylazine, 15 mg/kg) and perfused intracardially with 0.01 M PBS, pH 7.4, and 4 % paraformaldehyde (PFA). The spinal cord was dissected, post-fixed in 4 % PFA for 16 h, and cryoprotected in 20% sucrose overnight at 4 °C. Tissues were subsequently cut into 18 µm-thick sections, adhered to Superfrost Plus slides (Fisher Scientific), and frozen at −20°C. Samples were processed according to the manufacturer's instructions in the RNAscope Fluorescent Multiplex Assay v2 manual for fixed frozen tissue (Advanced Cell Diagnostics), and coverslipped with Fluoromount-G antifade reagent (Southern Biotech) with DAPI (Molecular Probes). The following probes, purchased from Advanced Cell Diagnostics were used: *Grpr* (nucleotide target region 463-1596; *GenBank*: NM_008177.2) and *Oprk1* (nucleotide target region 256 - 1457; *GenBank*: NM_001204371.1). Sections were subsequently imaged on a Nikon C2+ confocal microscope (Nikon Instruments, Inc.) in three channels with a 20X objective lens. Positive signals were identified as three punctate dots present in the nucleus and/or cytoplasm. For *Grpr/Oprk1* mRNA co-localization, dots associated with single DAPI stained nuclei were assessed as being co-localized. Images were taken across the entirety of the population of GRPR neurons in each spinal cord section. Cell counting was done by a person who was blinded to the experimental design.

Intra-spinal Virus Injection for Labeling GRPR Neurons

An IRES-iCre-Neo cassette was knocked-in to the 3'UTR of *Grpr* locus to generate *Grpr*^{iCre} mice (details of knock-in strategy will be published in a subsequent study). For spinal injection, *Grpr*^{iCre} mice were anesthetized with ketamine (90 mg/kg) and xylazine (10 mg/kg) intraperitoneally and injected with buprenorphine (BupSR, 0.5 mg/kg) for analgesia. Cervical vertebrae were exposed at C3-C6 and the vertebral column was mounted onto a stereotaxic frame with spinal adaptor (Stoelting catalog number: 51690). After removal of tissue around and between the vertebrae to expose the spinal cord, the dura was incised with a sharp needle to expose the spinal cord surface. AAV5-Ef1a-DIO-eYFP (5.6 X 10^{12} vg/mL) was injected into the left side of the spinal cord at 2 sites between successive vertebrae at C4-C5 with a Hamilton Neuros-syringe with beveled needle (catalog number: 65458-02, 34 gauge, 20 degree angle). The syringe needle was inserted into the dorsal spinal cord at an angle of ~35 degrees at a depth of ~250 µm to target the superficial dorsal horn. The AAV was injected (~500 nL AAV per injection) at a rate of 100 nL/min with a Stoelting Quintessential Injector (QSI, catalog number: 53311) and the needle was slowly removed 5 min after the injection was complete. The surgery site was closed with nylon sutures and triple antibiotic ointment and lidocaine were applied to the skin. Antibiotics (enrofloxacin, 2.5 mg/kg) with saline were injected subcutaneously to prevent infection. Mice were monitored for recovery following surgery and were perfused 2-3 weeks later for immunohistochemistry (IHC).

ISH and Immunohistochemistry (IHC)
ISH was performed using digoxigenin-labeled cRNA probes as previously described (Chen et al., 2001). IHC staining was performed as described (Zhao et al., 2014b). Briefly, mice were anesthetized with an overdose of a ketamine/xylazine cocktail and fixed by intracardial perfusion of 0.01 M PBS (pH 7.4) and 4 % PFA. Spinal cord tissues were immediately removed, post-fixed in the same fixative for 2-4 h, and cryoprotected in 20 % sucrose solution overnight at 4 °C. Spinal cord tissues were frozen in OCT and sectioned at 20 µm thickness on a cryostat. Free floating sections were incubated in blocking solution containing 2 % donkey serum and 0.1 % Triton X-100 in PBS (PBS-T) for 2 h at room temperature. The sections were incubated with primary antibodies overnight at 4 °C, washed three times in PBS, incubated with secondary antibodies for 2 h at room temperature and washed three times. Sections were mounted on slides with Fluoromount G (Southern Biotech) and coverslips. The following primary antibodies were used: rabbit polyclonal PKCδ antibody, (1:500, catalog number: sc-213, Santa Cruz Biotechnology) and mouse monoclonal NeuN antibody (1:2000, catalog number: MAB377, Millipore). Secondary antibodies were purchased from Jackson ImmunoResearch Laboratories: FITC or Cy5 conjugated donkey anti-rabbit or anti-mouse IgG (FITC - 1.25 µg/ml; Cy5 - 0.5 µg/ml). Confocal images were taken using a Leica TCS SPE confocal microscope. Three mice per group and 18 lumbar sections across each group were used for statistical comparisons.

Dissociation of Dorsal Horn Neurons
Primary culture of spinal dorsal horn neurons was dissected and dissociated from 5-7 day-old C57BL/6J mice. Three mice were used for each experimental condition (Zhao et al., 2014a). After decapitation, laminectomy was performed and the dorsal horn of the spinal cord was dissected out with a razor blade. The dorsal horn, kept on ice during dissection was incubated in Neurobasal-A medium (Gibco) containing 30 µl papain (Worthington) at 37 °C for 20 min. The tissue was washed three times in Neurobasal-A medium, after which gentle trituration was performed using a flame polished glass pipette, and cells were filtered through a 40 µm nylon cell strainer (BD Falcon). The homogenate was centrifuged at 1,500 rpm for 5 min and the supernatant was discarded. The cell pellet was resuspended in 180 µl culture medium consisting of Neurobasal medium (Gibco, 92 % vol/vol), fetal bovine serum (Sigma, 2 % vol/vol), horse serum (Invitrogen, 2 % vol/vol), glutaMax (Invitrogen, 2 mM, 1 % vol/vol), B27 (Invitrogen, 2% vol/vol), penicillin/streptomycin (Gibco, 100 µg/ml) and plated onto 12-mm coverslips coated with poly-D-lysine. The medium was changed daily, and calcium imaging was performed 3-5 days after seeding.

Calcium Imaging
Calcium imaging was performed on a Nikon Eclipse Ti microscope using fura-2 AM (Invitrogen). Drugs were dissolved or diluted to the required concentrations (shown in Figure legends) in artificial cerebrospinal fluid (ACSF) buffer (in mM): NaCl 140, $CaCl_2$ 2.4, $MgCl_2$ 1.3, KCl 4, HEPES 10, glucose 5. Results are presented as a ratio (F340/F380) and a calcium calibration buffer kit (Invitrogen) was used to quantify intracellular Ca^{2+} concentrations.

Whole-cell Phosphorylation Assays in HEK293 Cells
HEK293 cells expressing FLAG-KOR and Myc-GRPR were incubated in 10 µM U-50,488 or 1 µM PMA at 37°C, and lysed as described (Liu et al., 2011). Cells were lysed for 30 min at 4 °C in radioimmunoprecipitation (RIPA) buffer (50 mM Tris-HCl, 7.4; 1 mM EDTA; 1 % NP-40; 150 mM NaCl; 0.25 % sodium-deoxycholate; 0.1 % SDS) supplemented with protease inhibitors (0.5 mM PMSF, 1 µg/ml aprotinin, 1 µg/ml leupeptin, 1 µg/ml pepstatin) and a phosphatase inhibitor cocktail (Thermo Scientific). Solubilized lysates were cleared by centrifugation at 1,000 g for 5 min to remove nuclei and debris. A portion of the supernatants was removed and used to determine protein concentrations using Pierce® BCA Protein Assay Kit (Thermo Scientific). Cell lysates (supernatant fraction, S1) were incubated with Protein A/G PLUS agarose (Santa Cruz Biotechnology) and 1 µg immunoprecipitation antibody (mouse anti-Myc, catalog number: M4439) overnight at 4 °C. The resin was then collected by centrifugation, washed 4 times with 1 % NP-40 lysis buffer (50 mM Tris-HCl, 7.4, 1 % NP-40, 150 mM NaCl) and 3 times with 0.3 % PBST-2 (PBS + 0.3 % Triton X100). Bound proteins were eluted with Laemmli sample buffer (Bio-rad) supplemented with 50 mM dithiothreitol (DTT), heated for 10 min at 95 °C, and centrifuged at 10,000 xg for 5 min. The supernatant was loaded and resolved on a 7.5 % polyacrylamide gel (Bio-rad), and proteins were transferred to PVDF membranes (Millipore). Blots were blocked with 5 % w/v nonfat dry milk in PBS with 0.1 % v/v Tween 20 (PBST-3) and incubated overnight at 4 °C with mouse anti-phosphoserine antibody, Sigma (1:2500, catalog number P5747). The blots were then washed, incubated with donkey anti-mouse IgG-HRP antibody (Santa Cruz Biotechnology) at room temperature for 1 h, and detected by enhanced chemiluminescence (Thermo Scientific). Protein bands were analyzed by densitometry using Kodak 1D 3.6.

PKC Translocation Assay
HEK293 cells expressing KOR and GRPR grown in 29 mm glass bottom dishes (In Vitro Scientific) were transfected with pEGFP/PKCδ-eGFP or pEGFP/PKCα-eGFP (kindly provided by Dr. Peter M. Blumbergtaken) using lipofectamine 3000 (Invitrogen). After 24 h, cells were analyzed and the subcellular distribution of eGFP-fused protein was recorded under a Leica TCS SPE confocal microscope. Sequential images of the same cell were collected at 1 min intervals. Percent membrane translocation was calculated as $(I_{total} - I_{cyto})/I_{total} \times 100$, where I_{total} represents the total cell fluorescence intensity and I_{cyto} is the fluorescence intensity in the cytoplasm and the nucleus.

RT-PCR
RT-PCR was performed as previously described with Fast-Start Universal SYBR Green Master (Roche Applied Science) (Liu et al., 2011; Liu et al., 2014). All samples were assayed in duplicates (heating at 95 °C for 10 s and at 60 °C for 30 s). Data was analyzed using the Comparative CT Method (StepOne Software version 2.2.2.), and the expression of target mRNA was normalized to the expression of *Actb* and *Gapdh*. The primers used are *Actinb*: forward 5'-TGTTACCAACTGGGACGACA-3'; reverse 5'-GGGGTGTTGAAGGTCTCAAA-3'
Gapdh: foward 5'-CCCAGCAAGGACACTGAGCAA-3'; reverse 5'-TTATGGGGGTCTGGGATGGAAA-3'
Prkcd: forward 5'-AGAGGGACCCTGACAAGAGG-3'; reverse 5'-GTTGCTGTAGTCTGAAGGGGA *Prkca*: forward 5'-CTGGTGCTTGGGTTGAATG-3'; reverse 5'-TAACTCCTGGGGCTGCAC-3'

Bioluminescence Resonance Energy Transfer (BRET)
HEK293 cells expressing KOR and GRPR were transiently transfected with RLuc-EPAC-Venus (1 µg), a cAMP BRET sensor. Emission signals from Renilla luciferase (RLuc) and Venus were measured simultaneously using a BRET1 filter set (475–30/535–30) on a Synergy H1 Hybrid Reader (BioTek) as described (Jiang et al., 2007).

Statistical Analysis
Behavioral tests, cell counting and molecular analysis counting were performed by observers blinded to treatments and genotypes of the mice used. Statistical comparisons were performed using one or two way ANOVA followed by post-hoc analysis when comparing three or more groups, paired or unpaired, two-tailed student's t-test when comparing two groups with a 95% confidence interval with Graphpad Prism 7 (version 7.03, GraphPad). Groups were considered significantly different if $p < 0.05$. A normality test was performed to confirm the data were normally distributed. Values are presented as the mean ± standard error of the mean (SEM).

Supplemental references
Chen, Z.F., Rebelo, S., White, F., Malmberg, A.B., Baba, H., Lima, D., Woolf, C.J., Basbaum, A.I., and Anderson, D.J. (2001). The paired homeodomain protein DRG11 is required for the projection of cutaneous sensory afferent fibers to the dorsal spinal cord. Neuron 31, 59-73.
Jiang, L.I., Collins, J., Davis, R., Lin, K.M., DeCamp, D., Roach, T., Hsueh, R., Rebres, R.A., Ross, E.M., Taussig, R., et al. (2007). Use of a cAMP BRET sensor to characterize a novel regulation of cAMP by the sphingosine 1-phosphate/G13 pathway. J Biol Chem 282, 10576-10584.
Liu, X.Y., Wan, L., Huo, F.Q., Barry, D., Li, H., Zhao, Z.Q., and Chen, Z.F. (2014). B-type natriuretic peptide is neither itch-specific nor functions upstream of the GRP-GRPR signaling pathway. Mol Pain 10, 4.
Sharifi, N., Diehl, N., Yaswen, L., Brennan, M.B., and Hochgeschwender, U. (2001). Generation of dynorphin knockout mice. Brain Res Mol Brain Res 86, 70-75.